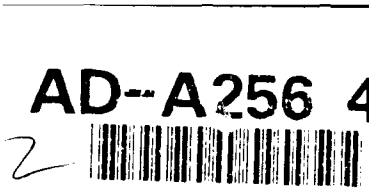

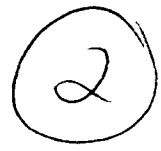

NAVAL POSTGRADUATE SCHOOL

Monterey, California

THESIS

Shiptrack Detection Algorithm Study

by

Vincent F. Giampaolo

June, 1992

Co-Advisor: Philip A. Durkee
Co-Advisor: Carlyle H. Wash

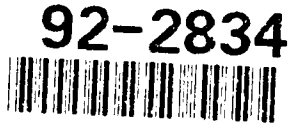

REPORT DOCUMENTATION PAGE

1a. REPORT SECURITY CLASSIFICATION Unclassified	1b. RESTRICTIVE MARKINGS
2a. SECURITY CLASSIFICATION AUTHORITY	3. DISTRIBUTION/AVAILABILITY OF REPORT Approved for public release; distribution is unlimited.
2b. DECLASSIFICATION/DOWNGRADING SCHEDULE	
4. PERFORMING ORGANIZATION REPORT NUMBER(S)	5. MONITORING ORGANIZATION REPORT NUMBER(S)
6a. NAME OF PERFORMING ORGANIZATION Naval Postgraduate School 6b. OFFICE SYMBOL (*If applicable*) 55	7a. NAME OF MONITORING ORGANIZATION Naval Postgraduate School
6c. ADDRESS (*City, State, and ZIP Code*) Monterey, CA 93943-5000	7b. ADDRESS (*City, State, and ZIP Code*) Monterey, CA 93943-5000
8a. NAME OF FUNDING/SPONSORING ORGANIZATION 8b. OFFICE SYMBOL (*If applicable*)	9. PROCUREMENT INSTRUMENT IDENTIFICATION NUMBER
8c. ADDRESS (*City, State, and ZIP Code*)	10. SOURCE OF FUNDING NUMBERS Program Element No. / Project No. / Task No. / Work Unit Accession Number
11. TITLE (*Include Security Classification*) Shiptrack Detection Algorithm Study	
12. PERSONAL AUTHOR(S) Giampaolo, Vincent F.	
13a. TYPE OF REPORT Master's Thesis 13b. TIME COVERED From To	14. DATE OF REPORT (*year, month, day*) June 1992 15. PAGE COUNT 104
16. SUPPLEMENTARY NOTATION The views expressed in this thesis are those of the author and do not reflect the official policy or position of the Department of Defense or the U.S. Government.	
17. COSATI CODES FIELD / GROUP / SUBGROUP	18. SUBJECT TERMS (*continue on reverse if necessary and identify by block number*) Shiptrack, Anomalous Cloud line, AVHRR

19. ABSTRACT (*continue on reverse if necessary and identify by block number*)

Shiptracks are known to be a relatively common phenomenon, often appearing in AVHRR channel 3 imagery as anomalous, curvilinear cloud lines. Despite their significance to remote ship surveillance studies, the formation mechanisms responsible for shiptrack production are still largely unknown and their specific characteristics still undefined. A shiptrack detection algorithm being developed here at the Naval Postgraduate School seeks to objectively detect and locate shiptracks on AVHRR imagery. This algorithm is a major step in objectively defining specific shiptrack characteristics and automating the search for additional shiptrack examples. The purpose of this study was to outline the logic of the detection algorithm and present a subjective performance summary of its usefulness. After careful analysis of the algorithm output files from several full satellite passes, it was determined that the algorithm is capable of detecting 65% of the fresh shiptracks within a full pass AVHRR image with a false detection rate of only 1.31 tracks per million square kilometers. This performance is likely to improve further with continued work focused on designing adequate filters to categorically reject many of the recurring false detections.

20. DISTRIBUTION/AVAILABILITY OF ABSTRACT ☒ UNCLASSIFIED/UNLIMITED ☐ SAME AS REPORT ☐ DTIC USERS	21. ABSTRACT SECURITY CLASSIFICATION Unclassified
22a. NAME OF RESPONSIBLE INDIVIDUAL Philip A. Durkee/Carlyle H. Wash	22b. TELEPHONE (*Include Area code*) (408) 646-3465/2295 22c. OFFICE SYMBOL 64De/64Wx

DD FORM 1473, 84 MAR 83 APR edition may be used until exhausted
All other editions are obsolete

Approved for public release; distribution is unlimited.

Shiptrack Detection Algorithm Study

by

Vincent F. Giampaolo
Lieutenant, United States Navy
B.S., The Ohio State University

Submitted in partial fulfillment
of the requirements for the degree of

MASTER OF SCIENCE IN METEOROLOGY AND OCEANOGRAPHY

from the

NAVAL POSTGRADUATE SCHOOL
June 1992

Author: _____
Vincent F. Giampaolo

Approved by: _____
Philip A. Durkee, Co-Advisor

_____
Carlyle H. Wash, Co-Advisor

_____
Robert L. Haney, Chairman
Department of Meterology

ABSTRACT

Shiptracks are known to be a relatively common phenomenon, often appearing in AVHRR channel 3 imagery as anomalous, curvilinear cloud lines. Despite their significance to remote ship surveillance studies, the formation mechanisms responsible for shiptrack production are still largely unknown and their specific characteristics still undefined.

A shiptrack detection algorithm being developed at the Naval Postgraduate School seeks to objectively detect and locate shiptracks on AVHRR imagery. This algorithm is a major step in objectively defining specific shiptrack characteristics and automating the search for additional shiptrack examples. The purpose of this study was to outline the logic of the detection algorithm and present a subjective performance summary of its usefulness.

After careful analysis of the algorithm output files on several full satellite passes, it was determined that the algorithm is capable of successfully detecting up to 65% of the fresh shiptracks within a full pass AVHRR image with a false detection rate of only 1.31 tracks per million square kilometers. This performance is likely to improve further with continued work focused on designing adequate filters to categorically reject many of the recurring false detections.

TABLE OF CONTENTS

ACKNOWLEDGEMENTS

I would like to extend a special thank you to Kurt Nielsen of the NavalPostgraduate School for his patience and support throughout this project. Kurt was responsible for writing the original algorithm and for taking the time to painstakingly help me dissect and analyze his work.

I am also grateful to Professors Philip Durkee and Carlyle Wash for their technical support and encouragement and of course to my wife (Amy) and daughter (Amanda) for their moral support on the home front.

I. INTRODUCTION

A. BACKGROUND

Anomalous cloud lines were first recognized in the summer of 1965 from a TIROS-IV (visible) satellite image southeast of the Kuril Islands. The image showed three long, plume-like cloud lines that crossed a large-scale cloud pattern at high angles, the longest of the cloud lines being 350 km long and 5 to 24 km wide. Careful inspection of the image suggested that the cloud lines were at an altitude near that of the large-scale band of clouds and were probably warmer than freezing. It was further suggested that their origin was anthropagenic, with possible sources given as stationary ships such as whaling vessels or factory ships that released large quantities of water vapor as they processed their catch at sea (Conover, 1966).

After conducting an exhaustive search for additional anomalous cloud line images, Conover published his conclusions on anomalous cloud line formation mechanisms based on the 16 known cases to date. He concluded that "the most likely cause of the cloud lines stems from exhaust from ocean going vessels. Large numbers of Aitken nuclei form in this exhaust. These are carried upward by the buoyancy of the hot gasses and "ship's air wake" to form droplets at slight supersaturation. This phenomenon does not appear related to special characteristics of the vessels power plant but to a critical condition of the atmosphere."

This early work demonstrated that under certain atmospheric conditions, the exhaust from ocean going vessels can result in the formation of anomalous cloud lines visible

from space in the visible wavelengths. It wasn't until 1987 however, when it was discovered that these same mechanisms produced similar cloud lines in pre-existing marine stratus clouds in the near infrared (3.7 μm), that the shiptrack phenomenon began to generate great interest from climatologists and more recently, leaders in Naval Intelligence.

This increased interest began when Coakley et al (1987) first described the shiptrack phenomenon based on observations made with NOAA Advanced Very High Resolution Radiometer (AVHRR) in the near-infrared and continued on into 1991 when a frequency of occurrence study off of the West Coast of the United States suggested that the phenomenon is relatively common in this high ship traffic density region, especially during the summer months (Durkee and Lutz, 1991). Coakley et al. observed that under stable meteorological conditions the effect of ship-stack exhaust on overlying marine stratus clouds is to increase the number of cloud droplets while decreasing the cloud droplet size, resulting in an increase in the reflectance of the cloud at 3.7 μm (and to a lesser extent 0.63 μm). Remote and in-situ measurements of shiptrack modified clouds made by Radke et al (1989) and Hindman et al (1990) indicate that the shiptracks contain a higher number of smaller cloud droplets and an increased liquid water content than the surrounding ambient cloud.

B. MOTIVATION

The formation mechanisms that produce shiptracks at sea are still not completely understood. Yet, when one looks at the effects that man-made aerosols have on the global climate, the shiptrack phenomenon may represent an effect several times more influential in modifying the local radiation budget than that of direct interaction of solar radiation with the ship produced aerosol particles themselves (Coakley et al, 1987). A thorough understanding of the effects of man-made aerosols on the reflectance of pre-existing clouds and their associated effects on the radiation budget is fundamental in completely understanding the effects of increasing levels of man-made aerosol emissions into the atmosphere. Essential to this understanding, and a logical place to focus the study, is in determining the necessary atmospheric conditions and formation mechanisms that produce shiptracks.

Shiptracks generally appear in near-infrared (near-IR) imagery, centered at 3.7 μm, as bright, curvilinear anomalies within marine stratiform clouds (Fig. 1). They tend to maintain a fairly constant width and brightness despite their persistence over several hundreds of kilometers. They range in width from roughly 7 to 10 km near their head and up to 25 km towards their trailing ends. In visible (VIS) imagery, centered at 0.63 μm, the same shiptracks do not always stand out, often appearing only slightly brighter than the surrounding cloud (Fig. 2). Finally, in infrared imagery (IR), centered at 11.0 μm, shiptracks do not appear at all. Cloud regions where shiptracks are known to be appear simply as ordinary medium to low level stratiform clouds in the infrared (Fig. 3).

Figure 1. AVHRR channel 3 image taken by NOAA-9 on July 13, 1987

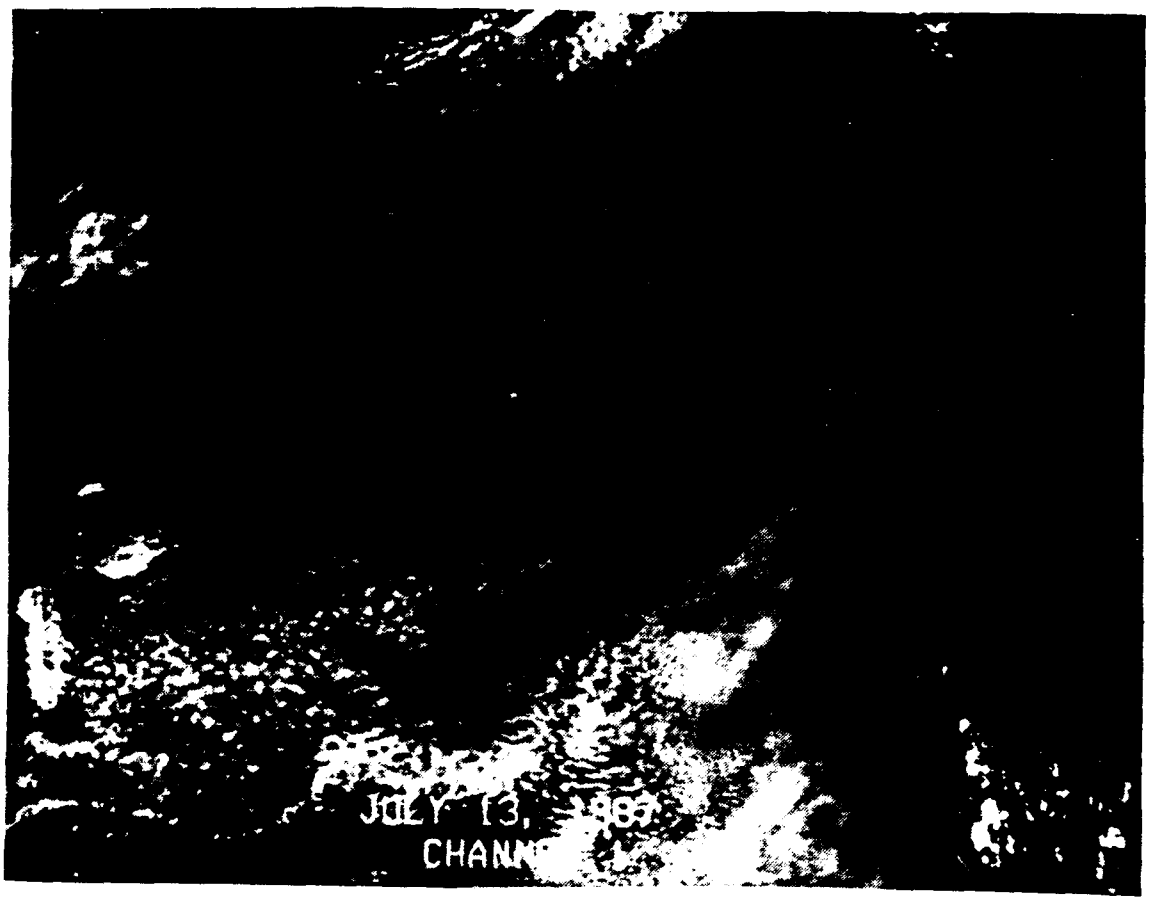

Figure 2. AVHRR channel 1 image taken by NOAA-9 on July 13, 1987

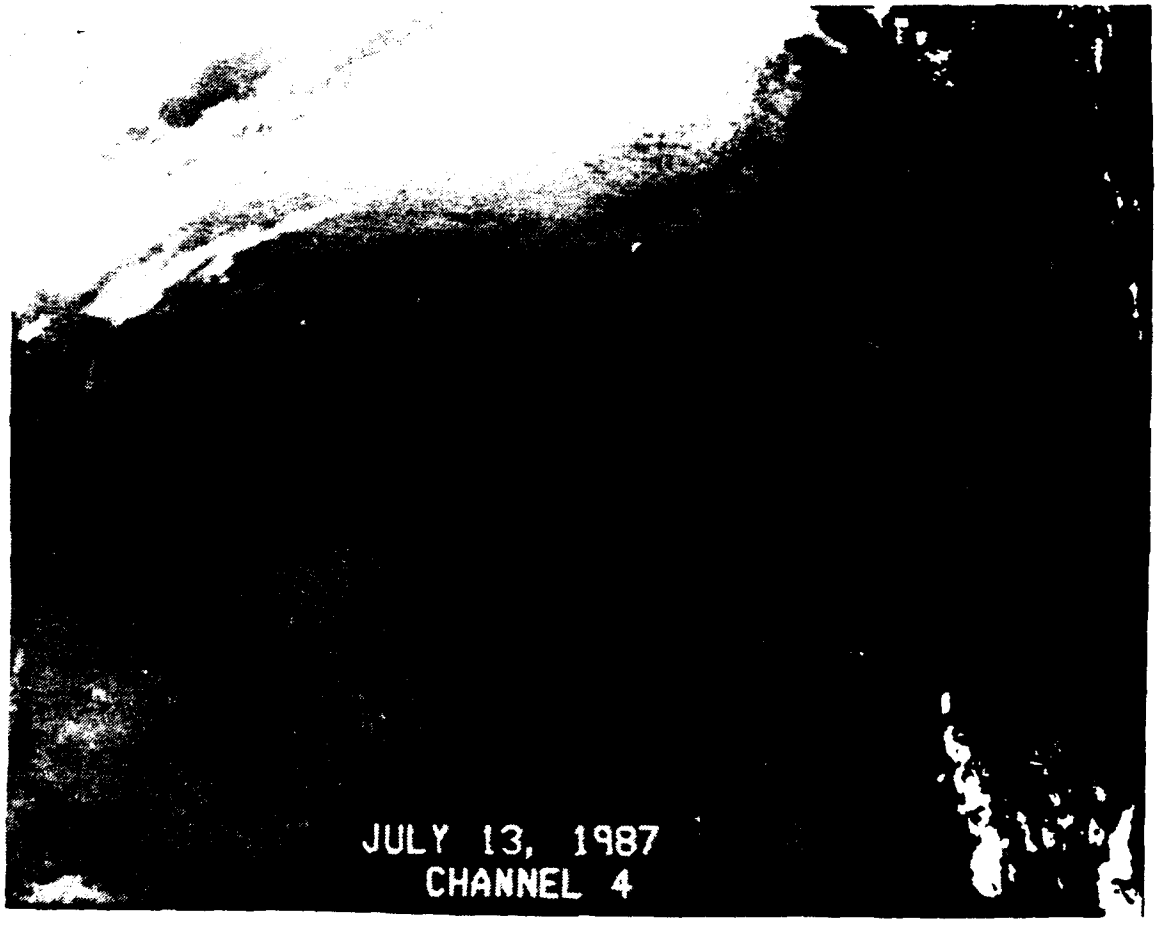

Figure 3. AVHRR channel 4 image taken by NOAA-9 on July 13, 1987

The shiptrack phenomenon is of particular interest to the Navy for its potential applications in remote ship surveillance. Until recently, potential enemy battle group movements could be detected from space only during daylight hours and under clear skies. Because shiptracks can be seen in marine stratus clouds in the near-infrared, they present an opportunity to fill in some of the time and area gaps in relocating a battle group lost under cloud cover. With the present technology shiptracks can only be used to approximate ship traffic density, individual ship positions and their relative courses and speeds. It is hoped that a thorough study of shiptracks will reveal an exploitable, long range, detection method for certain ship classes (i.e. size and/or powerplant) along with possible counter-detection procedures for our own forces.

C. OBJECTIVES

Shiptracks, like all cloud features, are extremely diverse. Distinguishing a shiptrack from the surrounding cloud features can often be very subjective, especially in regions where the clouds have naturally occurring sharp, linear features. It becomes more difficult to follow a shiptrack further away from its head. This subjectivity emphasizes the need to objectively define and locate shiptracks using characteristics of the image in the visible, near-infrared and infrared wavelengths. Removing the subjectivity in finding shiptracks is the first step in systematically analyzing and understanding shiptracks.

A second problem facing researchers is the time required to sift through the enormous quantity of satellite tapes to find a statistically valid number of shiptracks in which to base a study. Currently, an AVHRR satellite pass takes about 20 minutes to process

before it can be viewed. In order to get the resolution necessary to adequately see shiptrack features, the image must be blown-up (painted) frame by frame, often taking up to several hours to manually scan the entire image.

The most efficient way to objectively locate shiptracks on satellite images is by using a computer based shiptrack detection algorithm that can scan an entire satellite pass and use specific, known characteristics of shiptracks to distinguish the shiptracks from the surrounding cloud. One such algorithm is being developed here at the Naval Postgraduate School by Kurt Nielsen (under the direction of Professor Phil Durkee). It is the objective of this thesis to: 1) Outline the logic and various optional control parameter settings found in the current shiptrack detection algorithm, 2) Empirically determine the most efficient option settings of the algorithm based on a single, multiple-shiptrack satellite image and, 3) Present a performance summary of the algorithm on several AVHRR images.

II. SATELLITE DATA COLLECTION AND PROCESSING

The shiptrack detection algorithm is designed to work on Advanced Very High Resolution Radiometer (AVHRR), High Resolution Picture Transmission (HRPT), images taken from the National Oceanic and Atmospheric Administration (NOAA) polar orbiting satellites. The data stream is typically archived on standard 9-track magnetic tapes, each of which hold up to 7 minutes of data. Satellite images are processed from the raw data in the U.S. Naval Postgraduate School's Interactive Digital Environmental Analysis (IDEA) laboratory by a network of VAX 8250 computers. Once processed, the shiptrack detection algorithm can be run and the image viewed in full (at a reduced resolution) or in 512 x 512 pixel blocks (at full resolution).

A. SATELLITE

The current Polar Orbiting Operational Environmental Satellite (POES) flown by NOAA is the Advanced TIROS-N (ATN). The satellites themselves, two of which are flying at any given time, are in Sun-synchronous, circular orbits at altitudes of approximately 850 km. Under normal conditions, one satellite will be in an orbit with a southbound equator crossing time at about 0730 local solar time (LST), the other with a northbound equator crossing time at about 1430 LST. These orbits are selected to provide maximum global coverage within the limitations imposed by the communications and data handling facilities and the time-lines needs of data users (Rao et al. 1990).

The primary POES mission is to provide daily global observations of weather patterns and environmental conditions in the form of quantitative data usable for numerical weather analysis and prediction. POES spacecraft are used to observe and derive cloud cover, ice and snow coverage, surface temperatures, vertical temperature and humidity profiles.

B. SENSOR

The AVHRR is a scanning radiometer carried by the ATN that is sensitive to the VIS and near-IR, and IR "window" regions. Data is retained from a swath extending 55.4 degrees to either side of nadir (2048 pixels per scan per channel) having a resolution of 1.1 km directly below the satellite. The sensor records the Earth's radiation in five wavelengths, one in the visible, one in the near-visible and three in the infrared (Table 1). The data is transmitted to ground stations for distribution as 1.1 km resolution, High Resolution Picture Transmission (HRPT) data. Of particular interest to this study are the visible, near-infrared and thermal infrared HRPT data, (AVHRR channels 1, 3 and 4 respectively).

C. CHANNELS USED

In general, shiptracks are best seen in the near-IR channel 3 imagery. It is in this channel that all of the searching by the shiptrack detection algorithm for potential shiptracks occures. This channel is calibrated in units of radiance. Because channel 3 is in the near-IR, the daylight radiance observed from the satellite has contributions from both solar reflectance and thermal emission. By utilizing a method described by Allen (1987), the thermal emission portion of the total radiance at this wavelength can be subtracted out leaving only the reflected contribution. In this study, both types of channel 3 data are used and will be referred to as simply channel 3 data (solar reflectance and thermal emission) and Low3 (solar reflectance only).

The shiptrack detection algorithm uses data from channel 1(VIS) in various filter tests (which will be described in more detail in chapter 3) to help reject natural features which may look like shiptracks in channel 3 imagery. The data is calibrated in terms of albedo and is converted to units of percent reflectance. This conversion is based on weighting the received reflectance by the cosine of the solar zenith angle and the anisotropic reflectance factor (Allen, 1987).

The algorithm uses channel 4 (IR) data in much the same way it uses the channel 1 data. The data is the result of thermal emission and is converted to a radiance measurement with units of radiance by using a linear correlation to counts.

TABLE 1
AVHRR CHANNELS

CHANNEL	WAVELENGTHS(μm)	CENTER WAVELENGTH	PRIMARY USES
1	0.58-0.68	0.63	Daytime cloud/surface mapping
2	0.725-1.10	0.83	Surface water delineation, ice and snow melt
3	3.55-3.93	3.70	Sea surface temperature, night-time cloud mapping
4	10.30-11.30	11.00	Sea surface temperature, day/night cloud mapping
5	11.50-12.50	12.00	Sea surface temperature, day/night cloud mapping

III. SHIPTRACK DETECTION ALGORITHM

The goal of this chapter is to outline the processing steps, the detection logic and the sub-programs used to detect shiptracks. The shiptrack detection algorithm processes a full-pass AVHRR satellite image, using channel 1, 3 and 4 data to objectively locate shiptracks. The algorithm uses three (2048 x N pixels) files containing the channel 1, 3 and 4 data as inputs and returns a corresponding summary output file containing locations in the image where possible shiptracks can be found. The input files must be created using a program utility (called *Datadump)*, which converts the individual channel data from the satellite tapes to real data files, and a program (called *real2byte)* which then converts the real data files to a fixed record length byte file format that the algorithm can accept. The output file can be viewed directly by the user after it has been condensed to a 512 x 512 fixed record length file (using a program called *fixcond0)*. Once a satellite pass is loaded and processed, the steps taken to produce an output file can eventually become automated. This will allow the user to select a satellite pass overview, initiate the program, and come back several hours later to observe the results.

The detection code is composed of 13 separate modules which utilize 20 control parameters. This rather large computer program is required to do objectively what the human eye can do (albeit somewhat subjectively) at a glance. Shiptracks often stand out from their surroundings in channel 3 imagery as being long, curvilinear features of sharp contrasting brightness. Because the human eye can view an entire image at once, it is

able to fill in small gaps in the linearity where the shiptrack contrast with the surrounding cloud diminishes. With the present technology, it is not possible to reproduce what the eye can do so a rather complicated algorithm is required to enable a computer to detect shiptracks while only being able to process small sections of the image at a time.

A. THE LOGIC

The core of the program is a main do-loop which calls the 13 subroutines. Of these subroutines, 5 are administrative, dealing with such things as loading and manipulating the images and inputting the various control parameters, while the remaining 8 do most of the detection work. These 8 subroutines focus on detecting various generic shiptrack characteristics and ultimately pass their findings back to the administrative subroutines which record a shiptrack image onto a giant output image file. Due to memory limitations of the VAX computer, a main do-loop must break down the giant input images into 512 x 512 area images (hereafter referred to as block images) and feeds them one at a time to the subroutines for analysis. A shiptrack image file is created for each of the block images by the subroutines and passed back to the main program. A final subroutine is then called which maps the shiptrack image onto a giant output image file. This loop repeats itself until the entire giant input image is processed.

A detailed presentation of the algorithm logic is best handled by analyzing each subroutine separately in the order in which it is called by the main program. Since shiptracks are like long cloud "roads", construction terms are used to describe each

subroutine within the automated detection algorithm. The first call is to the subroutine *Foreman* which loads the user-selected control parameters into memory for use by the remaining subroutines inside the main do-loop. Once these settings are loaded, the program enters the main do-loop where the remaining subroutines are called to detect shiptracks and record their findings in the output file (Fig. 4).

1. Foreman

This subroutine finds and loads the 20 control parameters which are stored in a separate list file for easy manipulation. The parameters are listed in Table 2 along with the subroutine in which they are called and typical values of each parameter. Each of the parameters will be described in detail when the appropriate subroutine is discussed.

2. Getimg1, Getimg3, Getimg4

These subroutines read in block images from the giant channel 1, 3 and 4 byte files and map them into corresponding block files called IMG1, IMG3 and IMG4 respectively. *Getimg3* performs a conversion of the IMG3 data from byte to integer, resulting in a two dimensional array of integer channel 3 brightness values. IMG1 and IMG4 are initially left as byte arrays, which take up only 1/4 of the space of a corresponding integer array, and can be stored in this compact form until needed.

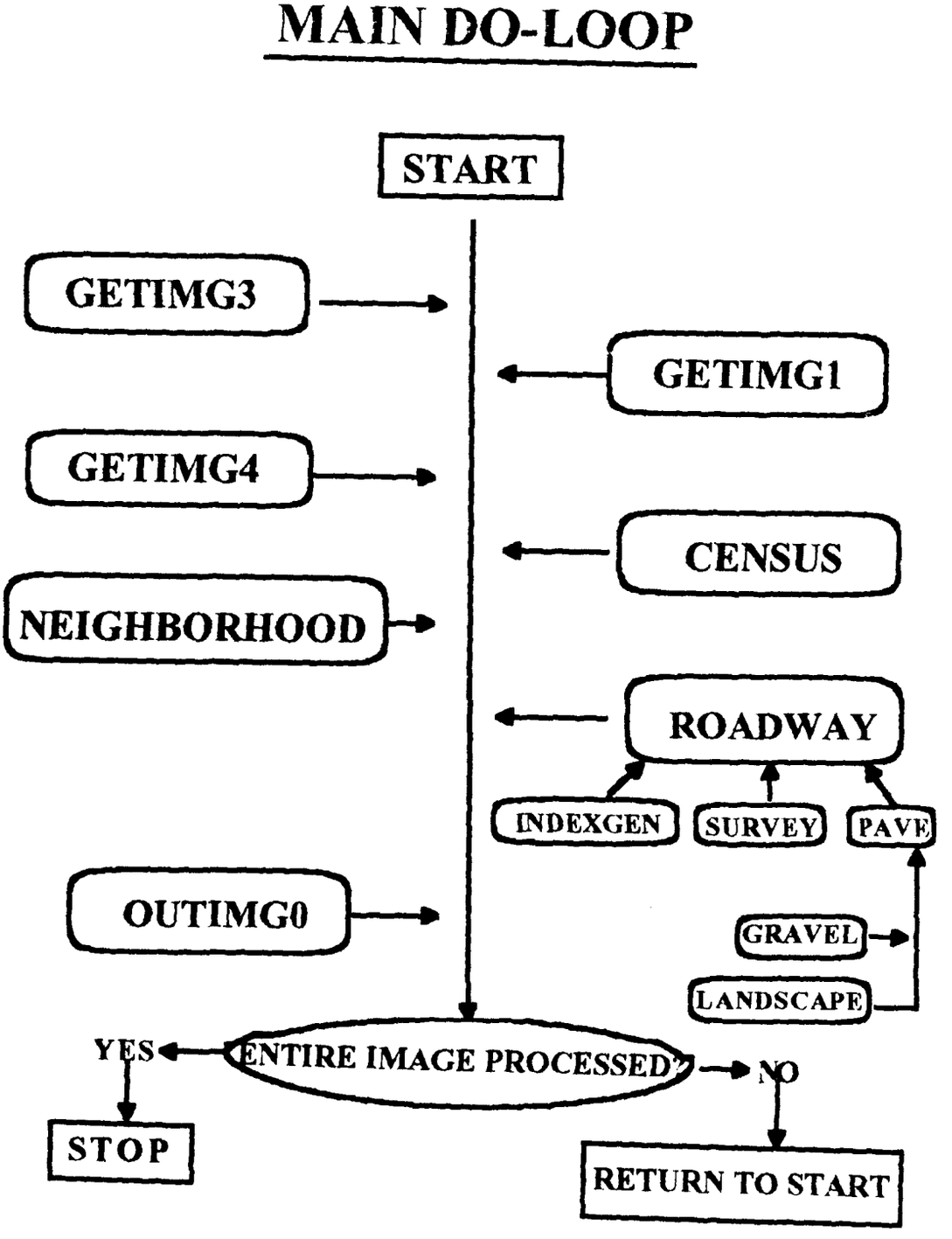

Figure 4. Shiptrack Detection Algorithm Main Do-Loop

TABLE 2
CONTROL PARAMETERS CALLED
IN SUBROUTINE FOREMAN

NAME	SUBROUTINE	TYPICAL VALUE
FACT	CENSUS	1.4
STDMIN	CENSUS	5
TLOW	CENSUS	273
THIGH	CENSUS	299
CUTOFF	NEIGHBORHOOD	8
RADIUS	ROADWAY	50
THRESH3(1)	PAVE	1
THRESH3(2)	PAVE	8
THRESH3(3)	PAVE	88
PATHRESH	PAVE	80
PATHGRAD	LANDSCAPE	8
THRESH3WD	LANDSCAPE	80
GRAV1	GRAVEL	70
GRAV2	GRAVEL	25
GRAV3	GRAVEL	10
GRAV4	GRAVEL	10
BOGUS1	GRAVEL	60
BOGUS2	GRAVEL	60
BOGUS5	GRAVEL	50
BOGUS6	GRAVEL	10

Conversion of the whole IMG3 array is done because the algorithm scans the entire channel 3 image looking for potential shiptrack features and requires channel 3 brightness counts (in integer form) for its initial search. The IMG1 and IMG4 array data are used in subsequent subroutine checks on prospective shiptrack features and are converted to integer form as needed.

3. Census

Census examines the IMG3 data and maps each pixel that exceeds certain brightness and temperature thresholds into an initially null giant working array (IMG0) as a code 1. Specifically the subroutine breaks the channel 3 block image up into 16 x 16 subareas and computes the mean and standard deviation for each. It then converts the corresponding subarea portion of the IMG4 array to integer form and calculates the temperature of each pixel. Provided the subarea has a sufficient variation in channel 3 pixel brightness (subarea standard deviation greater than *Stdmin*), each pixel within that subarea which has a channel 3 brightness count greater than the control parameter *fact* multiplied by the subarea standard deviation and a temperature within *Tlow* and *Thigh*, is flagged, and its position mapped as a code 1 in the working array. If the subarea standard deviation is below the control parameter *Stdmin*, the entire subarea is mapped as 0's in the working array.

4. Neighborhood

The neighborhood subroutine is designed to screen the "bright" pixels found in *Census* for randomness. Shiptracks tend to be long, linear, bright features in channel 3. If the "bright" pixels found in *Census* are randomly dispersed (ie, do not form linear patterns), they are likely not part of a shiptrack.

The subroutine breaks the working array (IMG0) into 16 x 16 subareas and counts each code 1 pixel. A separate 16 x 16 "neighborhood" array is created that maps the number of code 1 pixels located within +/- 2 pixel lengths from each pixel location in the IMG0 array. Pixels in IMG0 that have a corresponding "neighborhood" count in the neighborhood array that is greater than *Cutoff* are flagged and re-mapped as code 2's back in IMG0. This procedure ensures that only sufficiently "clumpy" bright areas are considered as potential shiptrack elements as opposed to randomly distributed bright pixels.

Finally a neighborhood representative is chosen from all of the code 2's within each subarea based on brightness. The brightest code 2 pixel within the subarea is flagged and re-mapped as a code 3 within IMG0. The end result is a working array of 1's, 2's and 3's, with the 3's being the essential information required by the next subroutine called *Roadway*.

5. Roadway

The objective of *Roadway* is to analyze path segments connecting neighborhood representatives to determine whether the segments meet certain criteria that are characteristic of shiptracks. The subroutine itself calls upon 5 of the remaining 6 subroutines and all (15) of the remaining control parameters used in the algorithm. Like *Census* and *Neighborhood*, *Roadway* uses IMG0 as the working array. Possible shiptrack path segments connecting the neighborhood representative (3's) are initially coded as 4's in an in-house array and are mapped as 5's in IMG0 if the paths are found to meet the various criteria defined by the control parameters to be discussed. The working array in this form is what makes up the output file of the algorithm. When an image is created using this information, the code 5 pixel locations can be viewed separately, marking the locations of algorithm-accepted shiptracks.

Roadway begins with a call to *Indexgen* (described below). It then begins scanning the block image line by line for neighborhood representatives (code 3 pixels). Once a representative is found, another search, centered on the representative, is conducted to look for other nearby representatives that may lie along a mutual shiptrack path segment. The search is conducted in the horizontal direction for plus or minus *Radius* pixel length units, and along the vertical (down direction only) *Radius* pixel length units for other code 3's. Once a potential shiptrack path is found, the coordinates of the representatives are passed on to *Survey* and *Pave* for analysis.

a. Indexgen

The bulk of the testing of potential shiptrack paths involves comparing the channel 1, 3 and 4 pixel values along the line between two neighborhoods to those of the adjacent cloud. This is done by marching along the pixel path between two neighborhoods, pixel by pixel, and comparing the local characteristics of the path to the cloud characteristics found on either side of, and directly perpendicular to, the path itself.

For each possible path orientation, the subsequent "testing" subroutines need to know the locations (or addresses) of the cloud pixels, out to a distance of 18 units in either direction, along the path perpendicular centered on each path point. To save each of the subsequent subroutines from having to compute these addresses each time, this is done only once in *Indexgen.*

Eight possible path perpendicular directions are considered for simplicity. For each of the eight directions, an array of relative adjacent cloud pixel addresses is computed and stored for ready access. This information is made available in the subsequent testing subroutines

b. Survey

Survey finds the addresses (image line and element) of each pair of neighborhood representatives that are sufficiently close to each other (described by control parameter *Radius*) to form a shiptrack path segment. The subroutine connects the representatives with a string of 4's, mapping each path out in a temporary memory space to be checked

by *Pave*. The orientation of each path are then computed and assigned one of eight possible orientation codes. These orientation codes are used to find the appropriate address array (computed by *Indexgen*) for the path perpendicular points used in the *Pave* checks.

c. Pave

Up to this point the algorithm has found sufficiently bright "neighborhoods" of pixels and, provided they were within a certain maximum distance apart, marked the paths between them as potential shiptrack segments (code 4's). *Pave* (with its subsequent calls to *Gravel* and *Landscape)* is where the actual testing of the potential paths occurs to determine if they exhibit properties (as defined by the control parameters) characteristic to shiptracks. These properties include brightness (channels 1and 3) and temperature differences with the adjacent cloud field and absolute brightness gradients in channels 1, 3 and 4.

Pave takes the addresses of neighborhood representatives that mark the ends of a possible shiptrack segment and the temporary roadway map generated by *Survey*. The subroutine then examines the path segment, one pixel at a time comparing the local cloud features along the path with those of the adjacent cloud found on both sides of the path. This is done by first loading the channel 3 brightness information of the adjacent cloud into a separate 2-dimensional array that is orientated in the same direction as the path itself (the orientation direction and the associated pixel addresses calculated by

Indexgen). The subroutine then examines each 1-dimensional path perpendicular array for each of the pixels along the path and performs brightness comparison tests between the different fixed subdivisions (Fig. 5) of the path perpendicular.

The average channel 3 brightness values are computed for each of the regions. For all but the Subfield region, these averages are computed by simply adding the pixel brightness values and dividing by the number of pixel units across. In the case of the Subfield region, a special bias is put in to help account for shiptracks that were significantly narrower than the subfield region itself. This bias effectively sets the subfield average to the average brightness value of any two or more pixels that both fall within the subfield region itself and are greater that the straight numerical brightness average within the region; essentially an average of the above average pixels. If there are not two or more pixels that meet this criterion, the subfield average is set to the simple numerical average brightness within the subfield region. Thus, when there is a significantly bright and narrow shiptrack, the subfield value used in the shiptrack path/adjacent cloud comparison tests is significantly brighter than the numerical average of the subfield pixels and is a better representative of the actual shiptrack than a simple numerical average of the subfield pixels.

Pave performs three simple channel 3 brightness comparison tests for each pixel along the path segment: 1) The subfield average must be brighter than the fullfield average by *Thresh3(1)* units, 2) The subfield average must be brighter than the nearfield average by *Thresh3(2)* units and, 3) The farfield average minus the nearfield

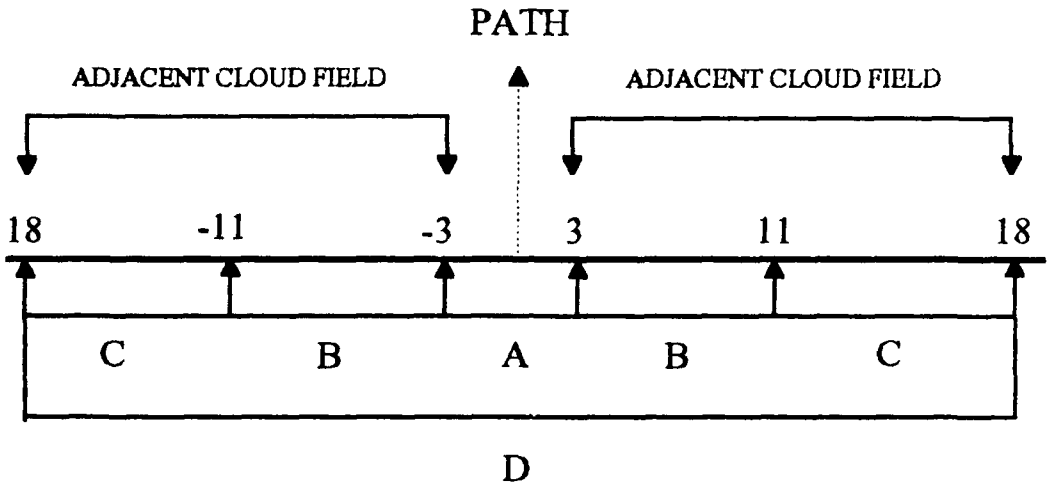

A = SUBFIELD

B = NEARFIELD

C = FARFIELD

D = FULLFIELD

Figure 5. *Pave* **path perpendicular subregions**

average must be less than *Thresh3(3)* units. If *Pathresh* percent of the pixels along the path segment pass all three of the above tests, the path is sent on to *Gravel* and then to *Landscape* for further testing.

1. Gravel

Gravel is designed to filter out natural quasi-linear IMG3 features that are actually gaps in the clouds, edges of continents or dense middle or high cloud shields. It uses channel 1 and 4 data to reject potential shiptrack features that exhibit sharp visible brightness gradients (cloud gaps), and/or sharp temperature gradients (continents or high cloud shield edges).

The subroutine looks at a 3 pixel wide region around each path segment point and a 4 pixel wide region symmetrically spaced on both sides of path along the path perpendicular. Within these regions, the channel 1 and 4 brightness values are averaged and used to compute several variables that are subsequently used in tests designed to accept or reject the path segment based on visible contrasts with the surrounding cloud and temperature and visible gradients. Figure 6 depicts the regions along each path perpendicular and Table 2 lists the variables computed from the channel 1 and 4 brightness values within those regions.

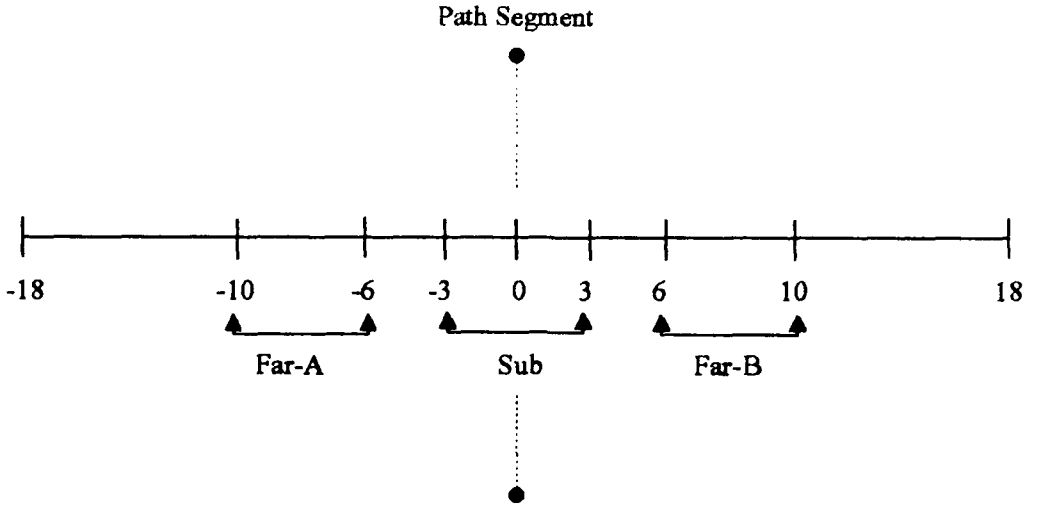

Figure 6. *Gravel* path perpendicular regions

TABLE 3
GRAVEL COMPUTATIONS

Variables computed for each path perpendicular

Sub1 = Average channel 1 brightness within the Sub region
Sub4 = Average channel 4 brightness within the sub region
Far1a (Far1b) = Average channel 1 brightness within Far-A (Far-B) region
Far4a (Far4b) = Average channel 4 brightness within Far-A (Far-B) region
Far1ave = (Far1a + Far1b) / 2
Far4ave = (Far4a + Far4b) / 2
Grad1 = Far1b - Far1a
Grad4 = Far4b - Far3a

Variables computed for the entire path segment

Grad1ave = Average channel 1path perpendicular gradient along the path
Grad4ave = Average channel 4 path perpendicular gradient along the path
Pathcount = The number of pixels along the path segment

The *Gravel* logic is best presented by way of a flow chart (Fig. 7). The sub-algorithm is entered with a potential shiptrack path segment and exited with an accept or reject flag that is sent back to *Pave*. Control parameters are shown in italics in the flow chart. *Grav1* is an absolute channel 1 brightness threshold. *Grav2, Grav3, Grav4, Bogus5* and *Bogus6* are channel 1 and 4 gradient thresholds. Finally, *Bogus1* and *Bogus2* are minimum accepted path perpendicular percentage values.

2. Landscape

Landscape is designed to analyze potential shiptrack path segments based on channel 3 brightness gradients characteristics. The idea is to force potential shiptrack path segments to be features confined by local channel 3 brightness gradient maxima and minima. Like *Gravel* , *Landscape* analyzes and tests single path segments passed on to it from *Pave*. The subroutine performs certain gradient tests on each path perpendicular and requires a minimum percentage of the path perpendiculars to pass before the decision is made to accept or reject the path segment.

The first thing that the subroutine does is reject path segments that are less than 20 pixels long. This filter is essentially an arbitrary CPU time saving step that was placed here in the last (and most recently added) subroutine to speed up the analysis. This restriction could have easily been placed in *Roadway* where a maximum path segment length limit of *Radius* pixels was imposed.

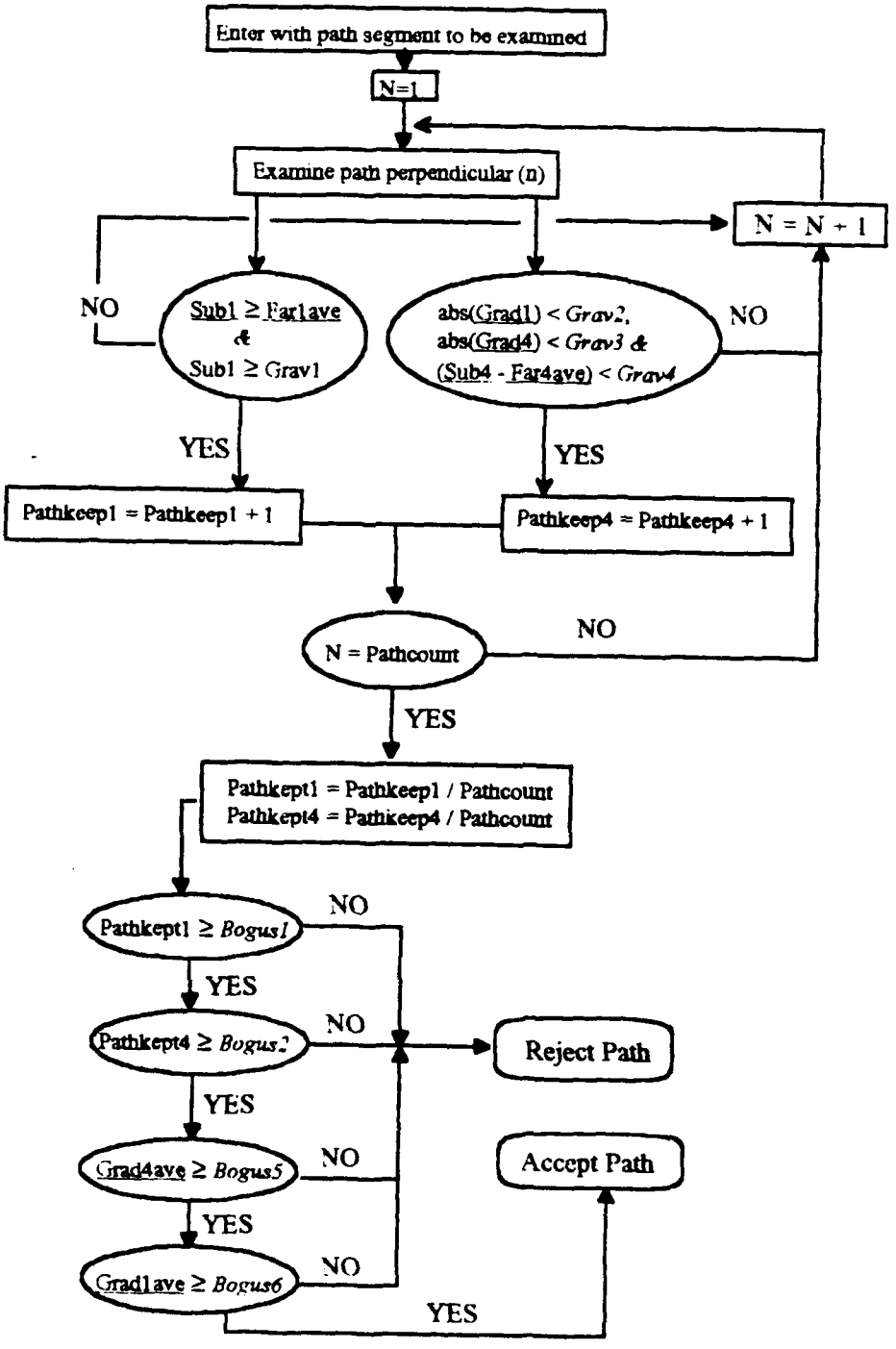

Figure 7. *Gravel* logic flowchart

The subroutine next sets out to compute the instantaneous channel 3 brightness gradient along each path perpendicular to define the path edges. The first step in this process is smoothing the brightness values along the path perpendicular. A three point running mean of the brightness values is computed from plus or minus 16 pixels from the path center. These smoothed brightness values are then used to compute a three point running gradient along the path perpendicular.

Once the instantaneous gradient is computed, the subroutine finds the local (plus or minus 9 pixels from the path center) gradient maximum and minimum. A restriction is then imposed on the path segments, requiring them to have one positive and one negative gradient extreme and that these gradient extremes have an absolute value which is greater than the control parameter *Pathgrad* but less than an arbitrary cutoff of 40.

The next restriction the subroutine places on the path perpendicular is to require the shiptrack path width to be greater than 3 pixels. This restriction is imposed to eliminate accepted path segments that are actually small scale gaps on either side of thin quasi-linear clouds. The path width is defined as the length between the gradient extremes plus 2 (Fig. 8).

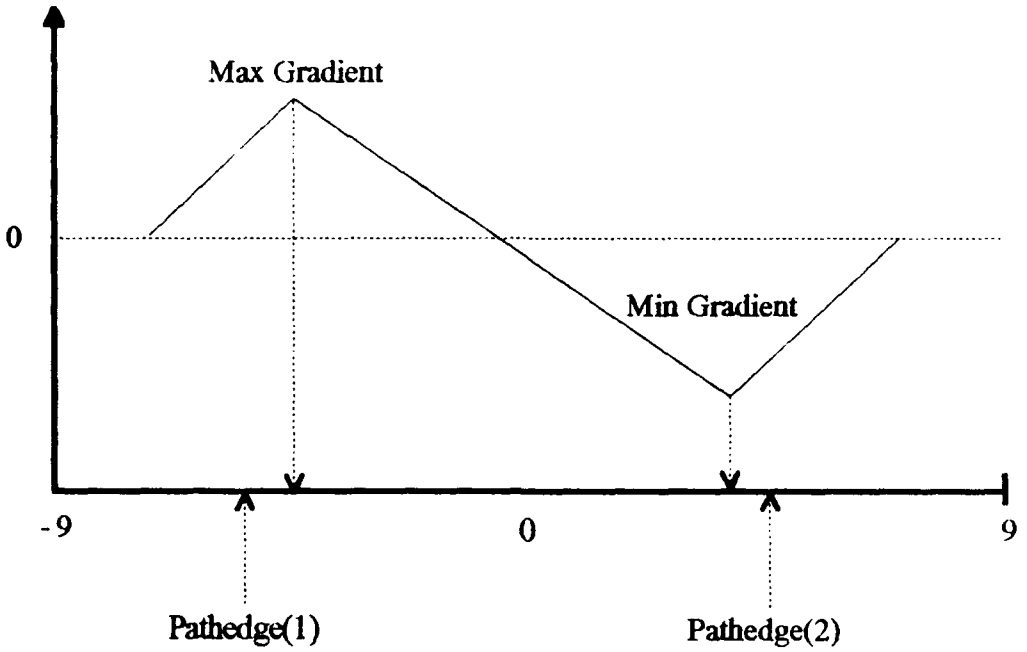

Figure 8. Landscape pathedges, arbitrarily set 1 pixel outward from the minimum and maximum gradients.

Next, the subroutine sets out to reject features having excessively noisy brightness gradients. This is done comparing the brightness gradients out to plus or minus 15 pixels from the center to the local (plus or minus 9) gradient extremes and rejecting those path perpendiculars which have more than one gradient greater than or equal to the local gradient extremes.

When the subroutine is through analyzing each path perpendicular, the percentage of those that passed the above test is computed. If this percentage is found to be greater than the control parameter *Thresh3wd*, the path is accepted, if not, it is rejected.

6. Outimg0

This subroutine is the final subroutine in the main do-loop. The working array is passed from the main program to *Outimg0* where it is written into the giant image output file in the corresponding positions to the original input files.

B. OUTPUT

The algorithm generates a giant integer output file containing a series of 2's, 3's and 5's. The 2's correspond to bright pixels on the original channel 3 image that stand out from their local surroundings. The 3's map local neighborhood representatives which mark the ends of potential shiptrack path segments and the 5's mark the connecting points between these end points. By using a condensing program (*fixcond0*) and a utility called *colors* (which can represent each of the three integers as a separate color), this output file can be easily viewed on the monitor or made into hard copies.

There are two ways to view the algorithm output with the original image to determine how well the particular run performed. The quickest and easiest way is to use a utility called *flicker* to rapidly alternate between the original and the output images on the monitor. The second option is to make hard copies of the original images and transparencies of the output image (both on the IDEA lab's RGBII laser printer) and overlay the transparency on the original image hard copy.

IV. PROCEDURES

As described in chapter three, the current shiptrack detection algorithm has 20 variable control parameters. Before a meaningful study could be conducted on the effectiveness of the algorithm at detecting shiptracks, a preliminary determination of the optimum settings had to be made. Once these settings were established, additional satellite passes were chosen and the algorithm run on each pass using the optimum settings. The runs were then separately analyzed and the effectiveness of the algorithm was subjectively determined for each.

The project was broken down into two phases. The first phase involved choosing a single satellite pass that contained multiple shiptracks of varying lengths, widths and brightness to be used as a baseline with which to test and optimize the algorithm settings. The shiptrack locations were manually (subjectively) determined on the image and multiple runs of the algorithm were made and compared to the subjective analysis. The optimum settings for the algorithm were determined based on the number of detections and false detections of each run.

The second phase of this study involved choosing additional satellite passes, subjectively determining the shiptrack locations and analyzing the results from each run of the algorithm (using the settings found in phase 1). The effectiveness of the algorithm was determined by comparing the subjective analysis to the objective analysis of the

algorithm by means of a series of statistical parameters developed specifically for this study.

A. PHASE 1

A satellite pass from NOAA-9 made on July 13, 1987 off of the West Coast of North America (Figs. 1, 2 and 3) was chosen as the initial test image because it was found to contain a large number of shiptracks of varying lengths, widths and brightness and covered a significantly large ocean area. Hard copies of these files were made using a Tektronix RGBII laser printer in the IDEA lab on which the shiptracks were located, numbered and highlighted manually.

Locating, highlighting and numbering the shiptracks on the hard copies was necessary in order to subjectively create a standardized image to be compared to each run of the algorithm. The procedure involved painting (an Avian utility where 512 x 512 portions of an overview are blown up in full resolution and viewed) the overview and hand drawing the shiptracks seen on the screen onto the hard copies. Locating the shiptracks on the monitor and then highlighting and numbering them on the hard copies was necessary due to the poor resolution of the hard copies themselves.

Each time the algorithm was run, a giant byte file was created. These files were converted to integer files and condensed, much like the giant image files were, using a program called *fixcond0*. By making transparencies of these output files and overlaying them on the image hard copies, the detections and false detections of each run were easily

and unambiguously noted. The optimum settings were selected based on the number of shiptracks detected and the number of false detections made.

With 20 control parameters available. in theory. a large number of possible setting combinations is possible. Fortunately, prior work on a previous 512 x 512 version of the algorithm established a few of the settings used in *Census* and *Neighborhood,* leaving 17 relatively untested parameters. An additional 3 parameters from *Gravel* were assumed to have only minimal effects on the algorithm efficiency and were left out of the testing. This left 14 untested control parameters that were assumed to play a major role in the algorithm efficiency (see Table 4).

B. PHASE 2

Once the optimum settings of the algorithm were determined, the attention was shifted towards testing the algorithm efficiency on suitable alternate satellite passes. The first image to be analyzed with the optimum settings after the original test image was a Low3 (vice channel 3) version of the original test image. Preparing this pass for the algorithm involved re-running the *Datadump* and *real2bye* programs to create a Low3, giant output file to be used instead of the channel 3 file. After the algorithm was run and the

TABLE 4
TESTED CONTROL PARAMETERS

Setting	Description	Subroutine
Thigh	Maximum channel 4 temperature reading of the potential shiptrack segment.	Census
Tlow	Minimum channel 4 temperature reading of the potential shiptrack segment.	Census
Radius	Maximum search radius to find connecting neighborhood representative.	Roadway
Thresh3(1)	Channel 3 path/full field minimum brightness contrast.	Pave
Thresh3(2)	Channel 3 sub/far field minimum brightness contrast.	Pave
Thresh3(3)	Channel 3 near/far field maximum brightness contrast.	Pave
Pathresh	Minimum percentage of path perpendiculars that must pass the Thresh3 tests.	Pave
Pathgrad	Minimum channel 3 brightness gradient across the path segment.	Landscape
Thresh3wd	Minimum percentage of path perpendiculars that must pass the Pathgrad test.	Landscape
Grav1	Minimum channel 1 brightness value of the potential shiptrack segment.	Gravel
Bogus1	Minimum percentage of path perpendiculars that pass pathkept 1 tests.	Gravel
Bogus2	Minimum percentage of path perpendiculars that pass pathkept 4 tests.	Gravel
Bogus5	Minimum path channel 4 gradient average	Gravel
Bogus6	Minimum path channel 1 gradient average	Gravel

subsequent analysis completed on this image, three additional passes were chosen and prepared in an identical manner to that in which the original test image was in phase 1. This preparation included creating the giant input files and hand drawing the shiptracks on the channel 3 image hard copies. Once the subjective analysis was complete on each pass, the detection algorithm was run and the output files analyzed.

Although the algorithm was not specifically designed to pick up any specific region of a generic shiptrack, during the analysis a distinction was made between the head region of a shiptrack the rest of the track segment. Shiptracks whose heads were visible on the image were categorized separately from those that did not, and shiptrack detections that included the head region of a shiptrack (to within a 20 km error margin) were noted. This emphasis on the shiptrack heads was done based on the assumption that the head of a shiptrack is the most recently formed part of the track and is therefore much less susceptible to dispersion and wind shears that influence the track down wind of the formation region. Additionally, the head, or formation region, of a shiptrack is the most critical part of the track for the purposes of both formation mechanism studies and ship to shiptrack correlation studies.

The analysis process involved collecting data from both the channel 3 and the algorithm output images and performing a series of simple statistical calculations intended to present the effectiveness of the algorithm on each run. The types of data collected on each run are listed in Table 5. The performance statistics developed to present the algorithm efficiency outlined in Table 6.

TABLE 5

DATA COLLECTED FOR EACH SATELLITE PASS

NS	=	◊Number of ST subjectively observed
NH	=	*Number of HT subjectively observed
SL	=	○Total length of observed ST
HL	=	○Total length of observed HT
OA	=	Total open ocean area in Km^2 x 10^6

DATA COLLECTED FOR EACH ALGORITHM RUN

STD	=	Number of ST objectively detected
HTD	=	Number of HT objectively detected
NHD	=	•Number of ST heads detected
STL	=	Total detected ST length
SHL	=	Total detected HT length
NFD	=	Number of false detections

◊ST = shiptracks
*HT = shiptracks with clearly visible heads
○Based on 1 pixel = 1.1 km
•Shiptrack detection within 20km of head location

TABLE 6
ALGORITHM PERFORMANCE STATISTICS

*ST detection rate (SR)	=	STD / NS
◊ STH detection rate (HR)	=	HTD / NH
ST length percentage (SL)	=	STL / SL
STH length percentage (HL)	=	SHL / HL
ST dectection confidence (SC)	=	STD / (STD + NFD)
False detection rate (FR)	=	NFD / (STD + NFD)
Head detection rate (HD)	=	NHD / STH
False detections per area (FD)	=	NFD / OA

* Denotes shiptrack
◊ Denotes shiptracks with clearly visible heads

V. RESULTS

A. PHASE 1

The objective of phase 1 of the project was to determine the optimum algorithm control parameter settings. The first step in determining how well any particular setting combination effects the algorithm's performance was creating a subjective shiptrack analysis from which to score each individual run. Such a standardized subjective shiptrack analysis was performed on the initial test image in accordance with the steps outlined in chapter 4. Channel 3 images of the northern and southern half of the original test image is presented in Figs. 9 and 10. Recall the northern half of this pass was used earlier to illustrate the appearance of shiptracks in the visible, near-IR and thermal-IR channels (Figs. 1, 2 and 3). The subjective shiptrack analysis for this pass is presented by Figs. 11 and 12. This analysis was then used as "ground truth" in scoring individual algorithm runs as described in chapter IV.

The next step in the project involved logically choosing appropriate control parameter setting combinations, running the algorithm and analyzing the results. By the time this study had begun, a 512 x 512 version of the basic algorithm had been in existence for almost a year and the optimum control parameter settings already generally determined. These initial settings provided a good starting point for the first phase of the project.

The initial objective of the first run of the algorithm on the test image was to determine how well the algorithm performed with the standardized control parameter settings. From the second run on, setting combinations were altered and/or internal modifications made to the code in an attempt to either improve specific performance characteristics or determine the effect an alteration of one or more of the control parameters had on the output. A separate 512 x 512 version of the algorithm was updated and was used to pre-check many of the changes on small regions of the full pass.

Table 7 outlines the specific performance results and control parameter settings of each run conducted in this phase of the research. Columns of Table 7 describe valid shiptrack detections (Det), false detections (F/D) and all of the tested control parameters discussed in chapters III and IV. Also shown are specific internal changes that were made to the algorithm between runs. In all, 18 runs of the algorithm were made, the last two of which were determined to present the optimum control parameter settings/internal code modifications for the algorithm.

The first of the internal modifications made, listed as "*Landscape* logic error" in Table 7, refers to a logic error that was found within the code that defaulted the main do-loop in the *Landscape* subroutine. The error caused *Landscape* to be more restrictive in its path acceptance tests than intended. On a run of the 512 x 512 version of the algorithm immediately following the logic error correction, the algorithm was found to be much less discriminating in its path segment testing, finding an increased number of valid shiptracks as well as false detections. This finding was confirmed on the full pass run

(number five) which found 28 valid shiptracks and produced 23 false detections. The increased number of false detections prompted a second series of internal modifications to the code intended to increase the algorithm's filter efficiency without sacrificing the valid detection rate.

The second internal change, listed as "*Gravel* modification" in Table 7, was an attempt to eliminate a specific recurring false detection off the coast of Southern California. The feature causing the false detection was an anomalously bright ridge in an otherwise broadly sloping brightness field of medium high cloud. The modification changed one of the path perpendicular requirements within *Gravel's* Pathkept1 tests (Fig. 7). Originally, each path perpendicular was required to have a Sub1 field brighter than Far1ave (Fig. 6 and Table 3). The change required that each path perpendicular have a Sub1 field brighter than both the Far-A and Far-B. This change was found to help eliminate certain false detections but overall produced an unacceptable decline in the valid shiptrack detection rate and was subsequently reversed.

The third change, listed as "*Landscape* modification" in Table 7, was made at the same time as the *Gravel* Modification (above) and refers to a lowering of the minimum pathwidth accepted in the Landscape subroutine from 5 to 3 pixels. This change was made in an attempt to allow the algorithm to pick up more shiptrack heads. The change was determined successful and was kept for all subsequent runs.

TABLE 7
PERFORMANCE SUMMARY AND
CONTROL PARAMETER SETTINGS
JULY 13, 1987 TEST IMAGE

Run	Det	F/D	A	B	C	D	E	F	G	H	I	J	K	L	M	N
1	22	8	278	291	50	1	8	88	80	8	80	-	-	-	-	-
2	30	16	278	291	50	2	8	88	80	8	80	70	60	60	50	10
3	27	8	273	299	50	2	8	88	80	8	80	70	60	60	50	10
4	27	10	273	299	45	1	5	90	75	5	70	70	60	60	50	10
								Landscape logic error corrected								
5	28	23	273	299	45	1	5	90	75	5	70	70	60	60	50	10
								Gravel/Landscape modifications made								
6	23	5	273	299	45	1	5	90	75	5	70	70	60	60	50	10
7	24	6	273	299	50	1	6	90	75	-	-	70	60	60	50	10
8	24	11	273	299	50	1	5	100	70	-	-	70	60	60	50	10
								Gravel modification reversed								
9	29	20	273	299	50	1	6	90	75	-	-	70	62	60	50	10
10	27	19	273	299	50	1	6	90	75	5	75	75	62	60	50	10
11	23	7	273	299	50	1	8	90	90	-	-	70	62	62	60	10
								New *Landscape* test added								
12	25	9	273	299	50	2	7	250	70	5	70	70	63	60	50	10
13	25	10	273	299	50	1	8	150	70	5	70	70	63	60	50	10
14	20	8	273	299	50	2	8	88	65	5	70	90	63	60	30	10
15	25	9	273	299	50	2	8	150	70	5	70	70	63	60	50	10
16	25	11	273	299	50	2	8	150	70	5	60	70	63	60	50	10
17	28	11	273	299	50	2	10	250	65	10	70	50	63	60	70	7
18	25	5	273	299	55	2	8	88	80	8	80	70	60	60	50	10

A = *Thigh*
B = *Tlow*
C = *Radius*
D = *Thresh3(1)*
E = *Thresh3(2)*
F = *Thresh3(3)*
G = *Pathresh*
H = *Pathgrad*
I = *Thresh3wd*
J = *Gravl*
K = *Bogus1*
L = *Bogus2*
M = *Bogus5*
N = *Bogus6*

*Blanks in columns H and I denote Landscape subroutine turned off

The last modification listed as "New *Landscape*" in Table 7, refers to a test added to the *Landscape* subroutine that rejects potential shiptrack path segments that have excessively noisy brightness gradients. This test was determined to be successful in increasing the *Landscape* filter efficiency and was kept for all following runs. The logic specifics of this test are described fully in the *Landscape* section of chapter III.

The final two runs conducted in phase 1 were selected as representing optimum control parameter settings based on the algorithm's performance on the single test image. Run 17 settings (hereafter referred to as Run A settings) produced a high number of detections with a moderate number of false detections (Figs. 13 and 14). This setting combination can be considered optimum when the number of false detections made by the algorithm is not as critical an issue as the number of detections. Run 18 (hereafter referred to as Run B) settings on the other hand produced a moderate number of false detections. The Run B setting combination was found to be the most conservative and could be used when the number of false detections is as least as critical as the number of detections made (Figs. 15 and 16).

The sub-algorithms which call the various control parameters that were tested in phase 2 can be thought of falling into two general categories: Those that search for potential shiptrack path segments and those that perform acceptance tests on the path segments found. Run A settings are designed to be somewhat relaxed in their shiptrack path segment search thresholds (Table 7 columns D through G) but relatively strict in their acceptance tests thresholds (Table 7 columns H through N). Recall from chapter III

that parameters D, E, and F are channel 3 brightness thresholds used in *Pave* to ensure potential shiptrack path segments are sufficiently brighter than the adjacent cloud field. Parameter G is the minimum percentage of the potential path segment that must meet these brightness criteria. Parameters H and I are used in *Landscape* as filter parameters. H is the minimum shiptrack pathedge gradient allowed by *Landscape* and I is the percentage of path perpendiculars that must meet the minimum gradient standards. The remaining parameters are used in *Gravel* (Fig 7). Parameter J is the minimum channel 1 brightness threshold of the shiptrack path segment. Parameters K and L represent the minimum percentage of the shiptrack path perpendicular that must meet the various channel 1 and 3 brightness and gradient tests. Finally, parameters M and N are the minimum average channel 1 and 4 path segment gradients.

In contrast to Run A, Run B settings are more strict in their search thresholds (D through G) but less restrictive in their acceptance test thresholds (H through N) than Run A. This difference in approach to finding valid shiptracks is the cause for the dissimilarities between the output runs using Run A and Run B settings.

B. PHASE 2

The additional satellite passes chosen for the second phase of the project came from the FIRE tape library in the IDEA lab. The images were taken by NOAA-9 and 10 in the summer of 1987 and are all centered off of the West Coast of North America. Specific dates are as follows: June 27, July 7, July 8.

1. Case study 1

The same July 13, 1987 pass that was used as the original test image in phase 1 was also used as the first case study in phase 2. Figures 9 and 10 are condensed (every fourth pixel) channel 3 images of the northern and southern halves of the full satellite pass. Although of reduced resolution, a majority of the shiptracks subjectively observed can be seen. Figures 11 and 12 show the subjective shiptrack analysis made on this pass, 11 being the northern and 12 the southern half. Tables 8 and 9 summarize the subjective and algorithm run findings for the channel 3 and low3 versions of the July 13 case study. Forty shiptracks were observed (NS) in the subjective analysis of this image, 23 of those falling into the category of having clearly defined heads (NH). Figures 13 and 14 show the algorithm (Run A settings) output for the northern and southern halves respectively. Overall Run A produced 39 detections, 28 of which corresponding to valid shiptracks (STD), and detected roughly 38% of the total shiptrack length (STL/ST). The Run B settings (Figs. 15 and 16) were slightly more conservative, producing 30 detections (25 of which corresponding to valid shiptracks) and detected roughly 31% of the total shiptrack length. Runs A and B on the low3 version of the pass (Table 9) did not score as well as their channel 3 counterparts, in each case producing a smaller number of detections while maintaining similar valid to false detection ratios. Detected tracks from the low3 version are illustrated on Figs. 17 through 20.

2. Case Study 2

The June 27 pass shows an extraordinary number of shiptracks concentrated in a relatively small area off of the coast of North America. A total of 52 shiptracks are observed, 44 of which had clearly visible heads. Figure 21 shows the condensed channel 3 image of the northern half of the pass (no shiptracks were observed in the southern half of the image) while Fig. 22 presents the subjective analysis made on that portion of the image.. Figures 23 and 24 are the algorithm output files from Runs A and B. Table 10 summarizes the findings from both the subjective analysis and the algorithm runs from this case study. Contrary to the findings in the first case study, both runs found the same number of valid shiptracks (STD=27), although not necessarily the same shiptracks, with Run A actually finding a fewer number of false detections (NFD=6) than Run B (NFD=7). Similar to the first case study however, Run A detected a higher percentage of total shiptrack length (STL/ST) than Run B (19% to 21% respectively).

3. Case study 3

In general, shiptracks did not appear on the July 7 pass. Although 19 shiptracks are subjectively observed, very few had the brightness and clarity observed in the previous two passes. Additionally, the image shows a large number of north-south running cloud edges in the low sun angle, southeast most portion of the image and consequently was an area of high false detections. Figures 25 and 26 show the condensed channel 3 images of the northern and southern halves of the pass respectively and Figs. 27 and 28 show the

subjective shiptrack analysis made on each. The reader should be reminded that the hard copy figures do not display all the detail of the digital data and the overview images have reduced resolution (every fourth pixel) compared to the complete subscene. Consequently many of the subtle shiptracks are not obvious in the overview figures. Run A (Figs. 29 and 30) produced a higher number of detections and found a greater percentage of total shiptrack length than Run B (Figs. 31 and 32). Run B, however, had a higher valid to false detections rate than did Run A. The specific findings of each run along with the subjective shiptrack analysis statistics are summarized in Table 11.

4. Case study 4

Figs. 33 and 34 show the condensed channel 3 images from the July 8 pass, northern and southern halves respectively. The subjective shiptrack analysis for these images are shown in figs. 35 and 36. Again, this image showed few bright and continuous shiptracks as compared with case studies 1 and 2. A total of 16 shiptracks were observed, 13 of which had clearly visible heads. Runs A (figs. 37 and 38) and B (figs. 39 and 40) performed slightly better than the July 7 and are summarized along with the subjective analysis statistics in Table 12.

5. Summary

The data outlined in the Tables 9 through 12 was used to compute the performance statistics as outlined in chapter IV. These statistics are presented in Table 13. The table

is broken down into Run A and B settings, last row in each section, labeled "combination", was computed using the combined number of shiptracks, shiptrack length etc. from each run within that section. The values in this column can be thought of as the weighted average value from each run.

In general, algorithm runs using Run A settings detected a higher percentage of shiptracks with clearly visible heads than Run B (65% and 58% respectively) and a greater percentage of these shiptrack lengths (26% and 23 %). At the same time however, Run A settings scored lower shiptrack confidence rates than Run B (63% to 72%), producing an average of 1.31 false detections per million square kilometers as compared to an average of only 0.87 false detection per million square kilometers for Run B settings.

C. FALSE DETECTIONS

Algorithm false detections per unit ocean area were pleasingly low. Many of the features causing false detections were small (usually under 50 km in length) but nonetheless fulfilled each of the algorithm objective shiptrack tests. A small handful of the features could not be identified and fell into a categorical description of anomalous cloud features. The majority of the remaining false detections fell into four general categories; 1) Cloud edges in low sun angle regions, 2) Thin, elongated stratoform clouds over water (especially near the edges of the satellite pass), 3) Gravity wave

interactions with the marine boundary layer, and 4) Old shiptrack remnants. Examples of the first three categories are given in figs. 41 through 43.

Figure 41 shows a full resolution (512 x 512 subscene) channel 1 and 3 image of a north-south running cloud edge in the low sun angle region of the July 7 pass. A bright, linear feature is clearly seen in the channel 3 image along the eastern edge of the low cloud centered in the image. This feature is on the same order of magnitude as a shiptrack and produced a false detection on both algorithm runs. Currently no adequate filter has been designed to stop the algorithm from detecting such features.

Figure 42 is a full resolution channel 1 and 3 image taken near the edge of the July 8 satellite pass. This image shows apparently thin bright clouds in both channels 1 and 3 surrounded by darker adjacent clouds. Because this view is at the edge of the satellite pass, the oblique view is grossly distorted and these clouds are actually much wider than they appear. This feature produced a false detection on both algorithm runs on the July 8 pass. A potential algorithm modification that would vary the maximum pixel width of accepted shiptracks as a function of the number of degrees off nadir the feature is located may provide a means of eliminating this particular problem.

Finally, Fig. 43 shows both a channel 1 and channel 3 full resolution image of gravity wave phenomenon off of the Baja Peninsula on the July 13 pass. Gravity waves force the upper saturated marine boundary layer to come in contact with the dryer air above in a sinusoidal pattern. As the saturated air comes in contact with the dryer air, the cloud droplets become smaller due to evaporation and consequently, the visible and

near-IR reflectance increases. This is seen in both the channel 1 and channel 3 images. This feature produced false detections on both algorithm runs.

Additional study of the reasons for false detections of shiptracks will produce better filters for the algorithm, allowing less restrictive shiptrack search parameters. This will ultimately lead to overall improvements in the algorithm's performance.

Figure 9. Northern half of July 13, 1987 AVHRR channel 3 image

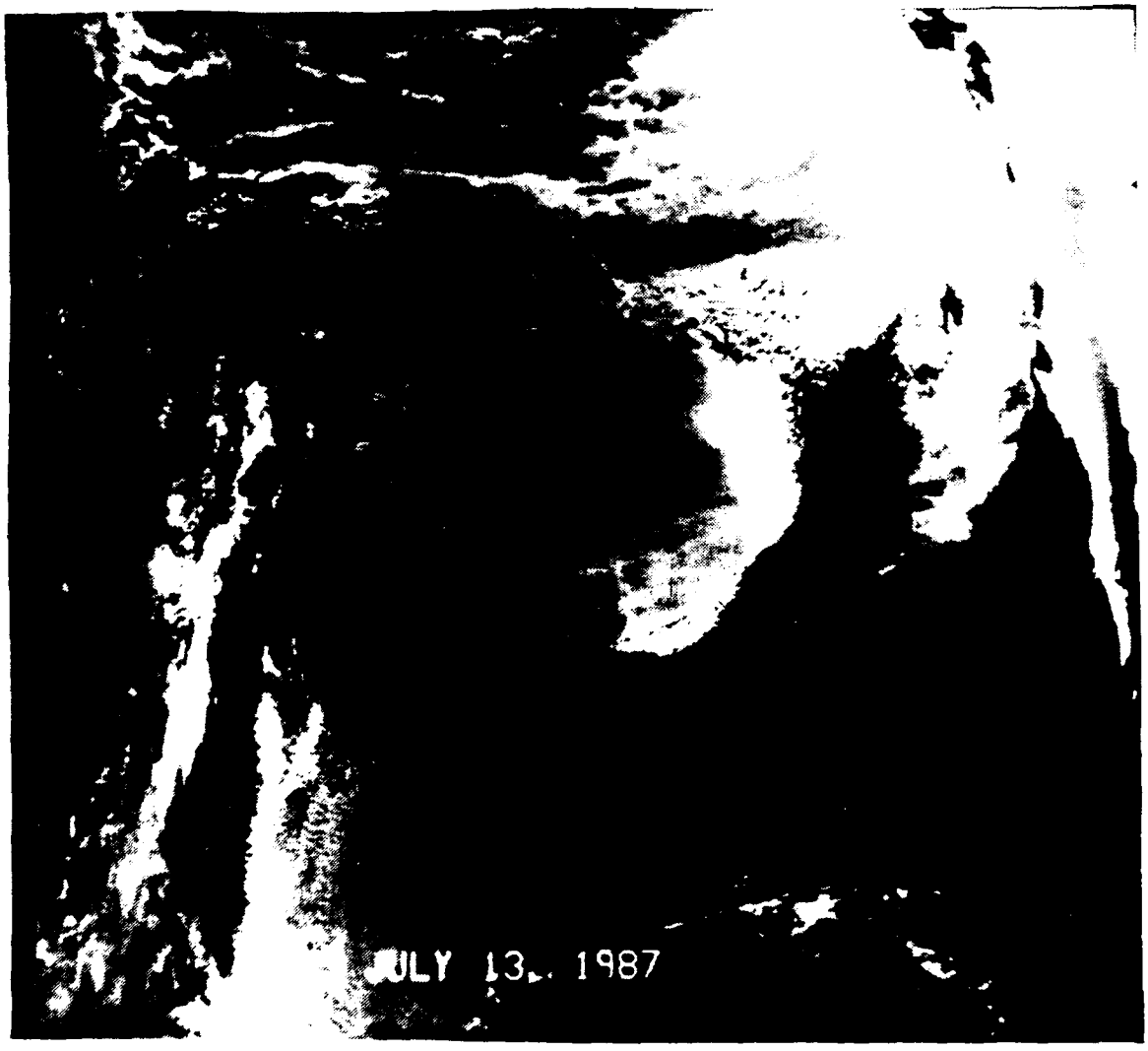

Figure 10. Southern half of July 13, 1987 AVHRR channel 3 image

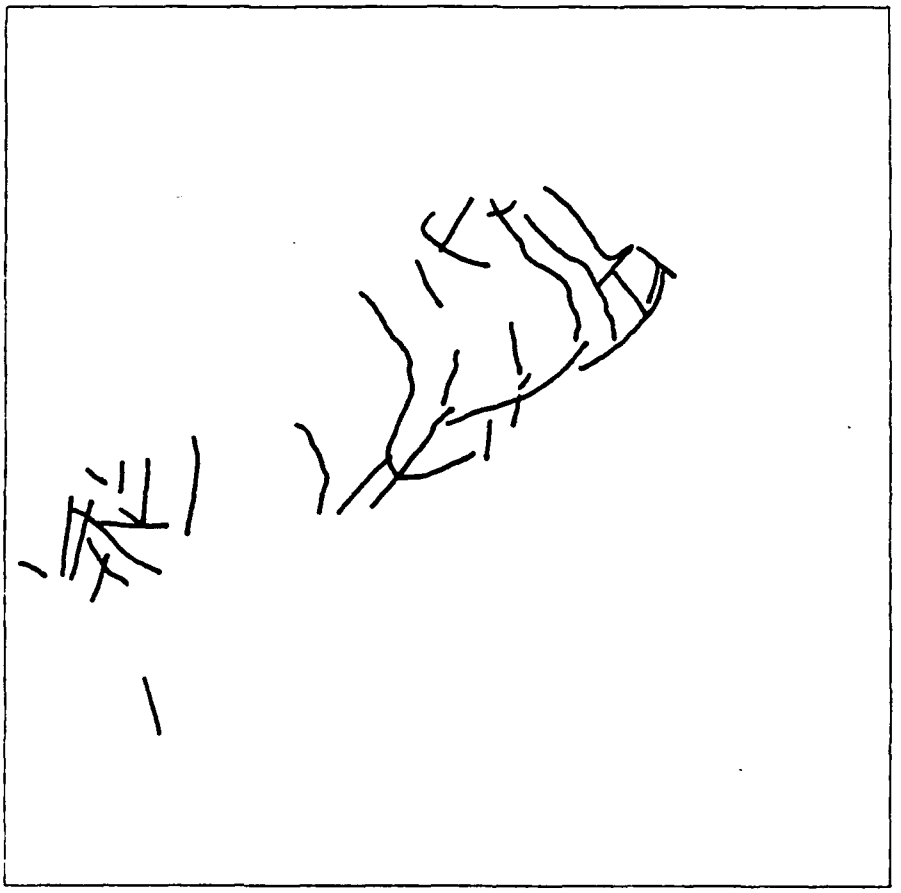

Figure 11. Subjective shiptrack analysis of northern half of July 13, 1987 pass

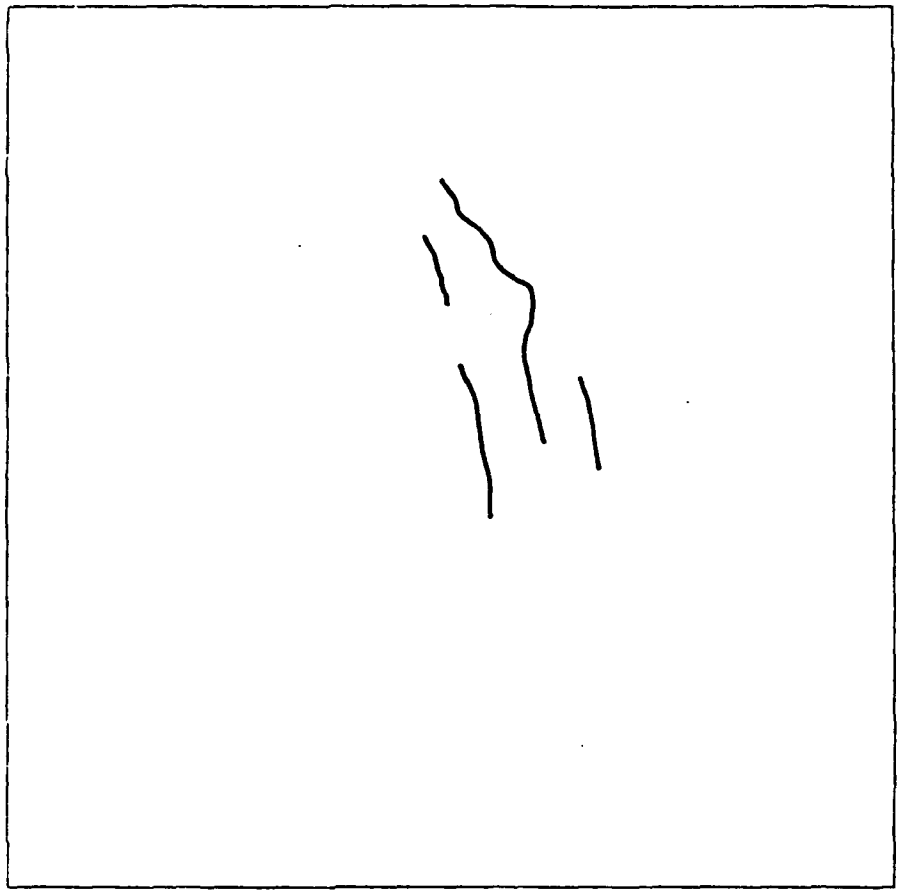

Figure 12. Subjective shiptrack analysis of southern half of July 13, 1987 pass

Figure 13. Algorithm Run A on northern half of July 13, 1987 pass.

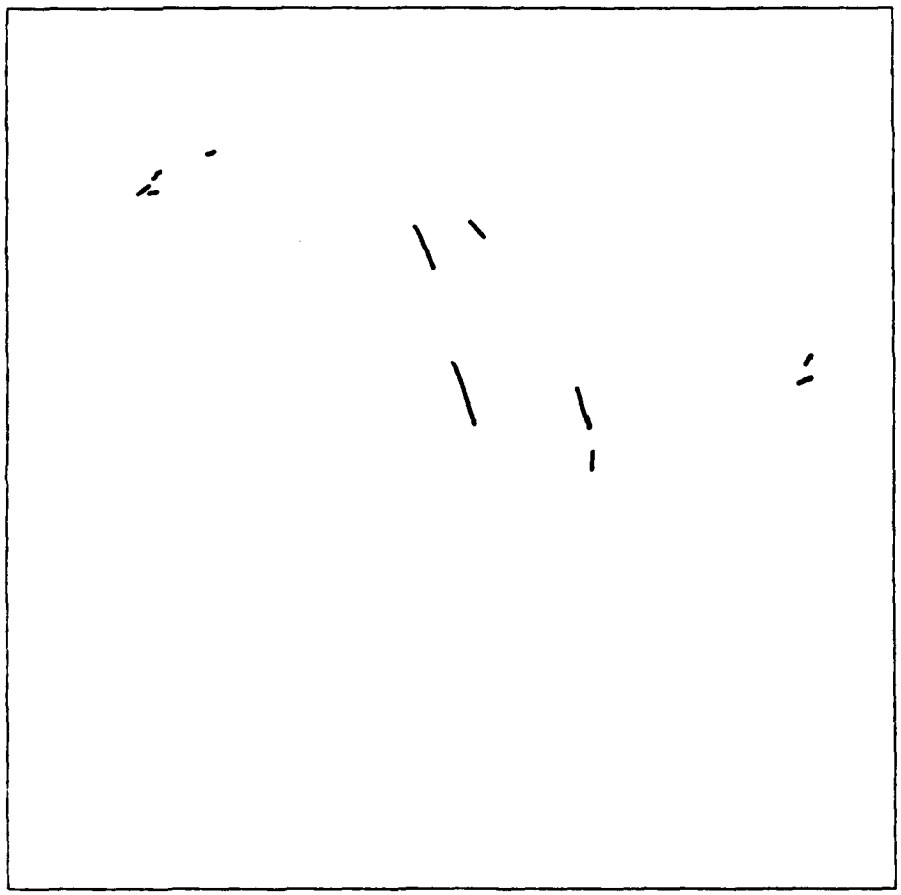

Figure 14. Algorithm Run A on southern half of July 13, 1987 pass.

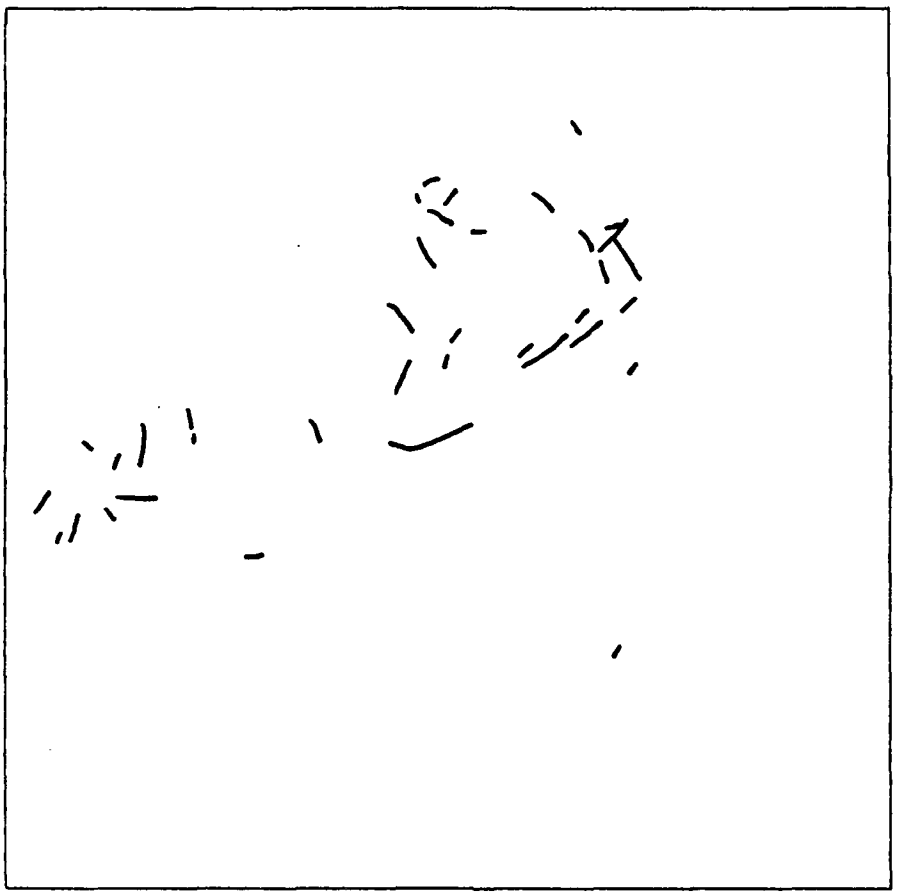

Figure 15. Algorithm Run B on northern half of July 13, 1987 pass.

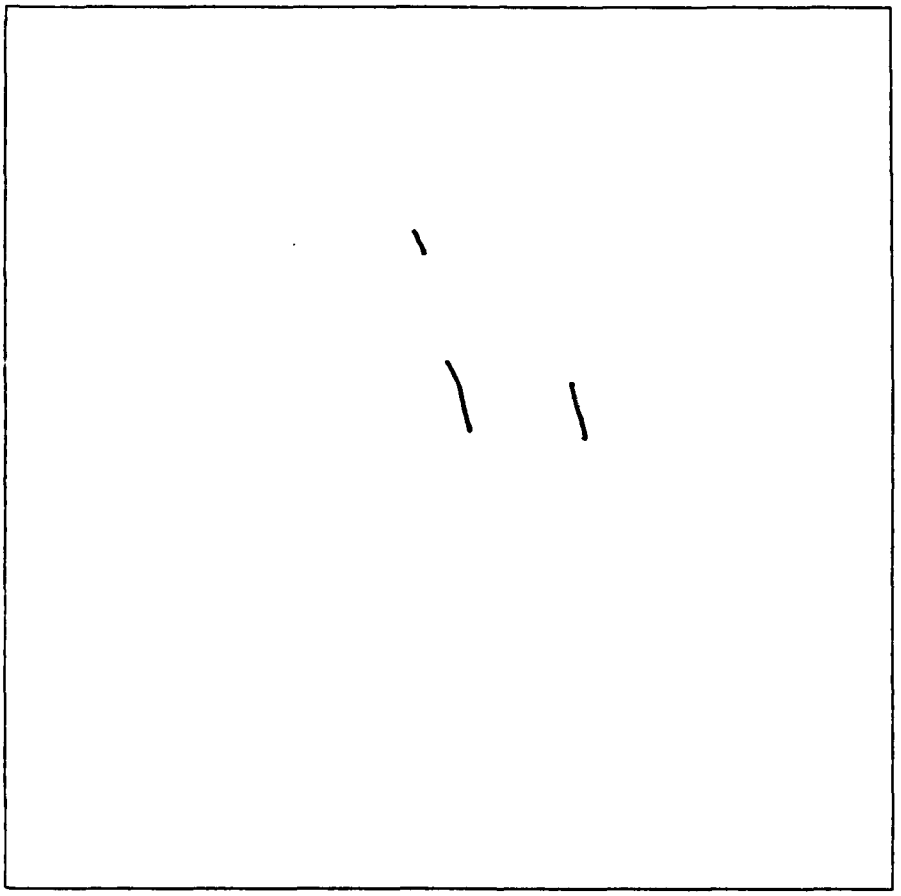

Figure 16. Algorithm Run B on southern half of July 13, 1987 pass.

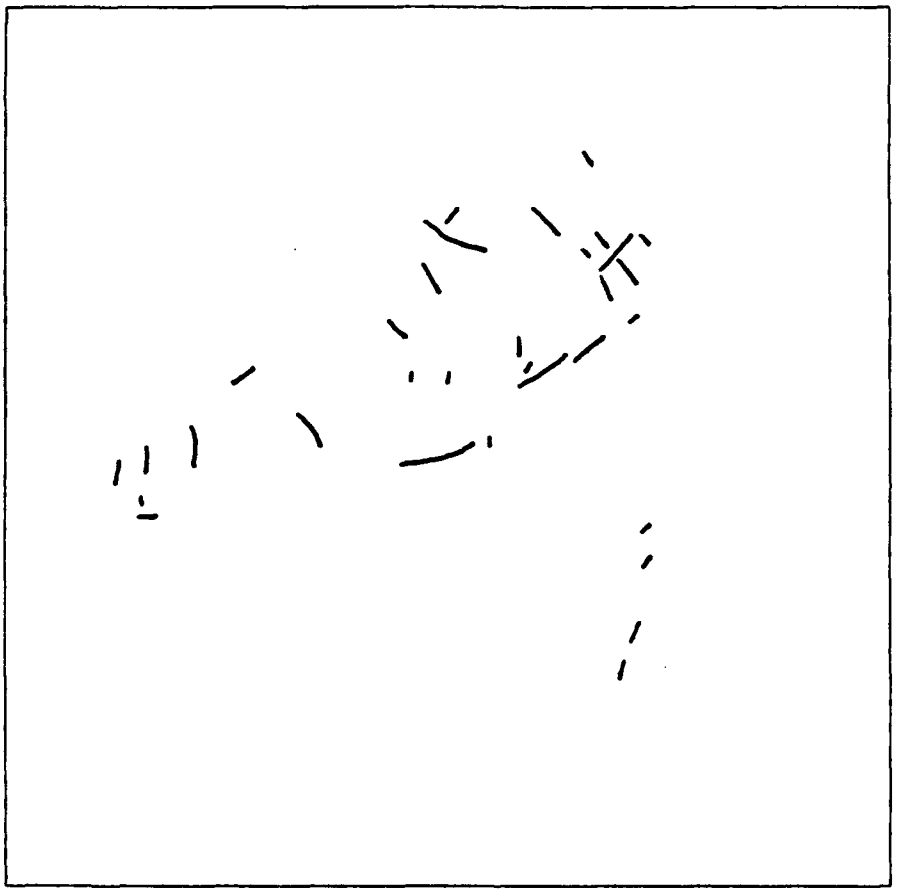

Figure 17. Algorithm Run A on Low3 version of northern half of July 13, 1987 pass

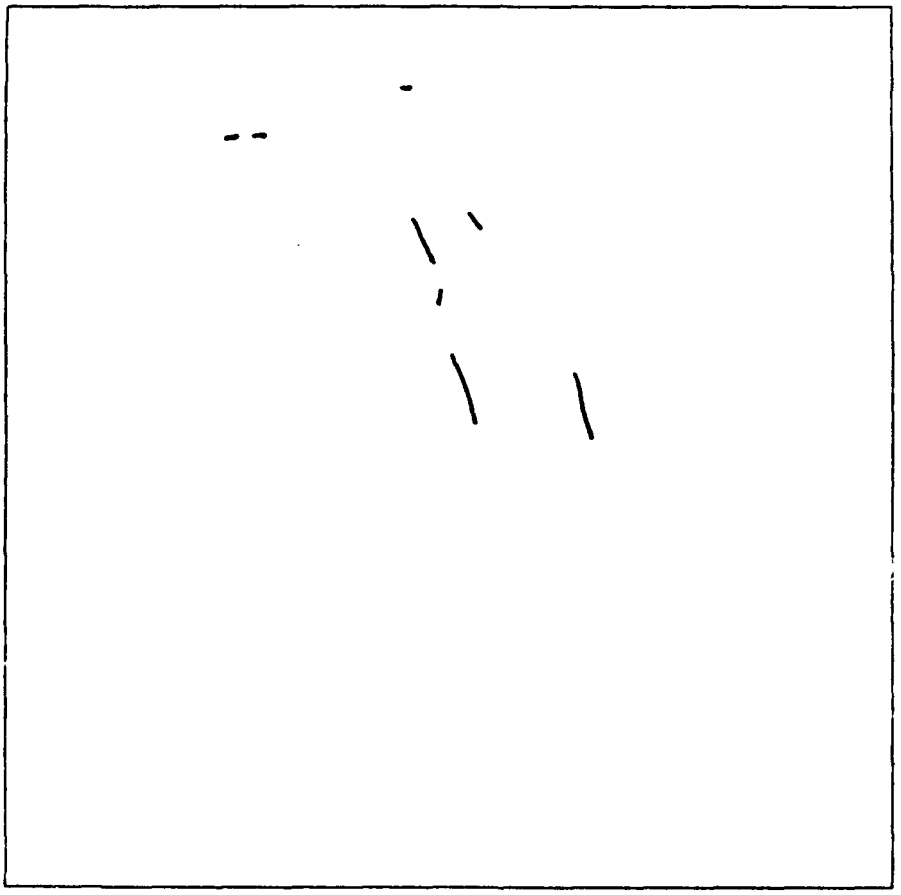

Figure 18. Algorithm Run A on Low3 version of southern half of July 13, 1987 pass

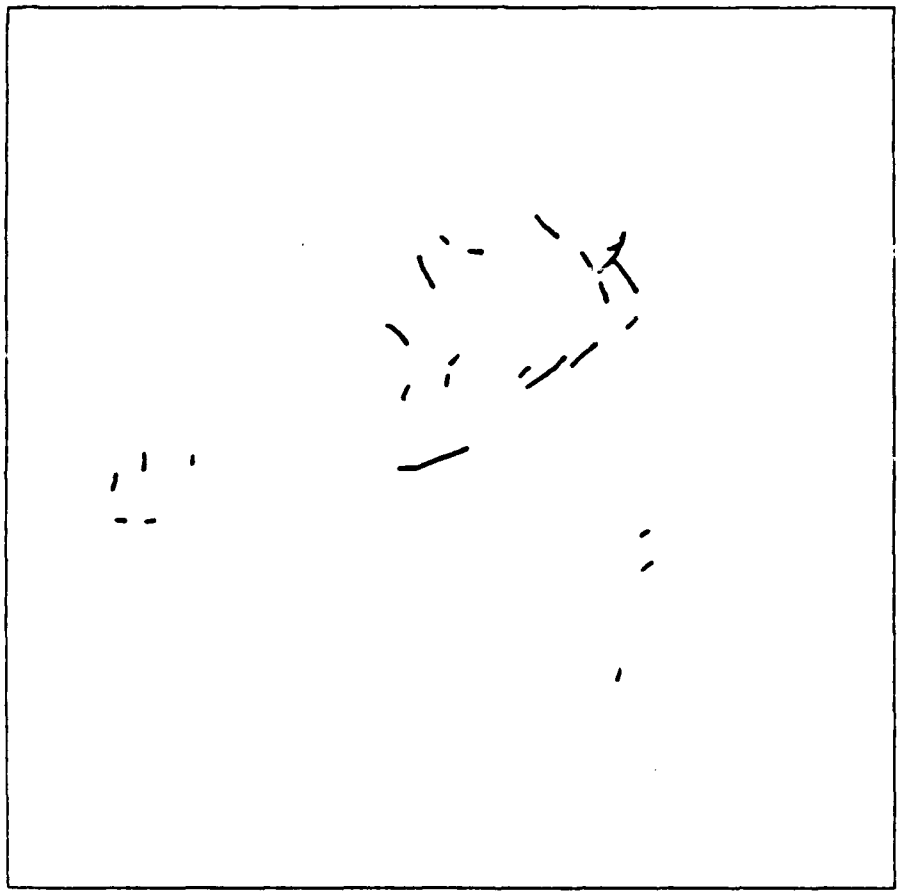

Figure 19. Algorithm Run B on Low3 version of northern half of July 13, 1987 pass

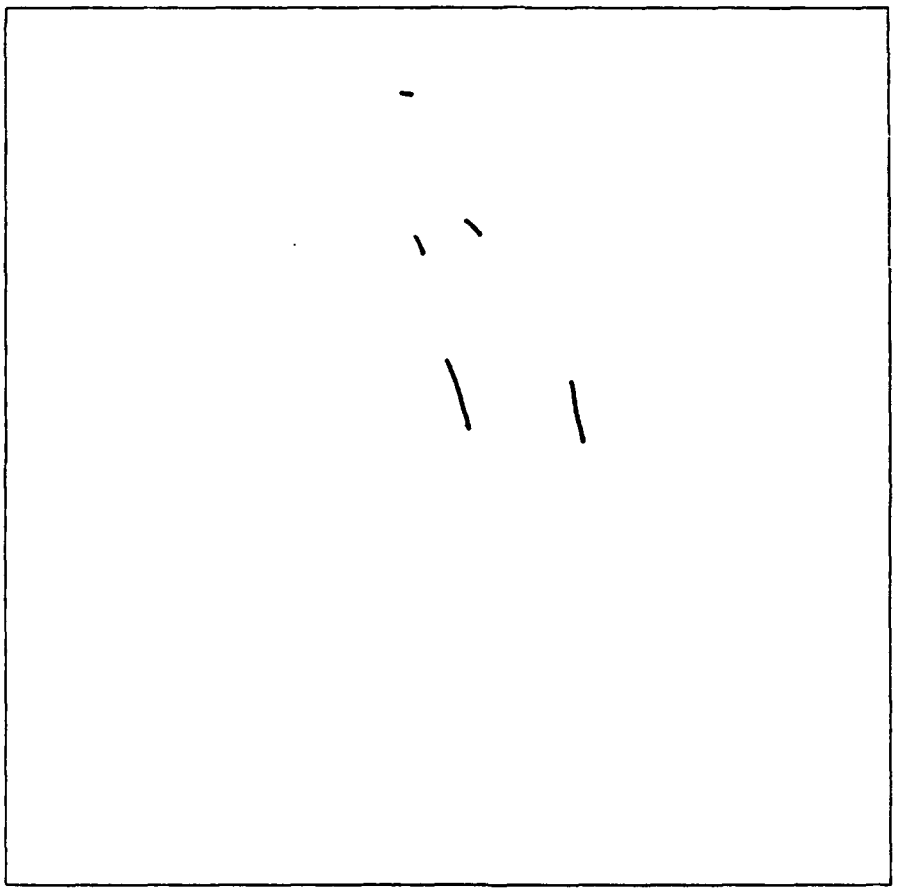

Figure 20. Algorithm Run B on Low3 version of southern half of July 13, 1987 pass

TABLE 8
JULY 13, 1987
SUBJECTIVE AND ALGORITHM
DETERMINED STATISTICS

SUBJECTIVE STATISTICS

NS = 40
NH = 23
ST = 8450
HL = 4680
OA =8.40

RUN A STATISTICS

STD = 28
HTD = 21
NHD = 16
STL = 3215
SHL = 2575
NFD = 11

RUN B STATISTICS

STD = 25
HTD = 18
NHD = 14
STL = 2595
SHL = 2015
NFD = 5

NS	=	Number of ST subjectively observed
NH	=	Number of HT subjectively observed
SL	=	Total length of observed ST
HL	=	Total length of observed HT
OA	=	Total open ocean area in $km^2 \times 10^6$
STD	=	Number of ST objectively detected
HTD	=	Number of HT objectively detected
NHD	=	Number of ST heads detected
STL	=	Total detected ST length
SHL	=	Total detected HT length
NFD	=	Number of false detections

TABLE 9
JULY 13, 1987 (LOW3)
SUBJECTIVE AND ALGORITHM
DETERMINED STATISTICS

SUBJECTIVE STATISTICS

NS = 40
NH = 23
ST = 8450
HL = 4680
OA = 8.40

RUN A STATISTICS

STD = 25
HTD = 19
NHD = 13
STL = 2645
SHL = 1625
NFD = 9

RUN B STATISTICS

STD = 20
HTD = 16
NHD = 11
STL = 2090
SHL = 1235
NFD = 4

NS	=	Number of ST subjectively observed
NH	=	Number of HT subjectively observed
SL	=	Total length of observed ST
HL	=	Total length of observed HT
OA	=	Total open ocean area in $km^2 \times 10^6$
STD	=	Number of ST objectively detected
HTD	=	Number of HT objectively detected
NHD	=	Number of ST heads detected
STL	=	Total detected ST length
SHL	=	Total detected HT length
NFD	=	Number of false detections

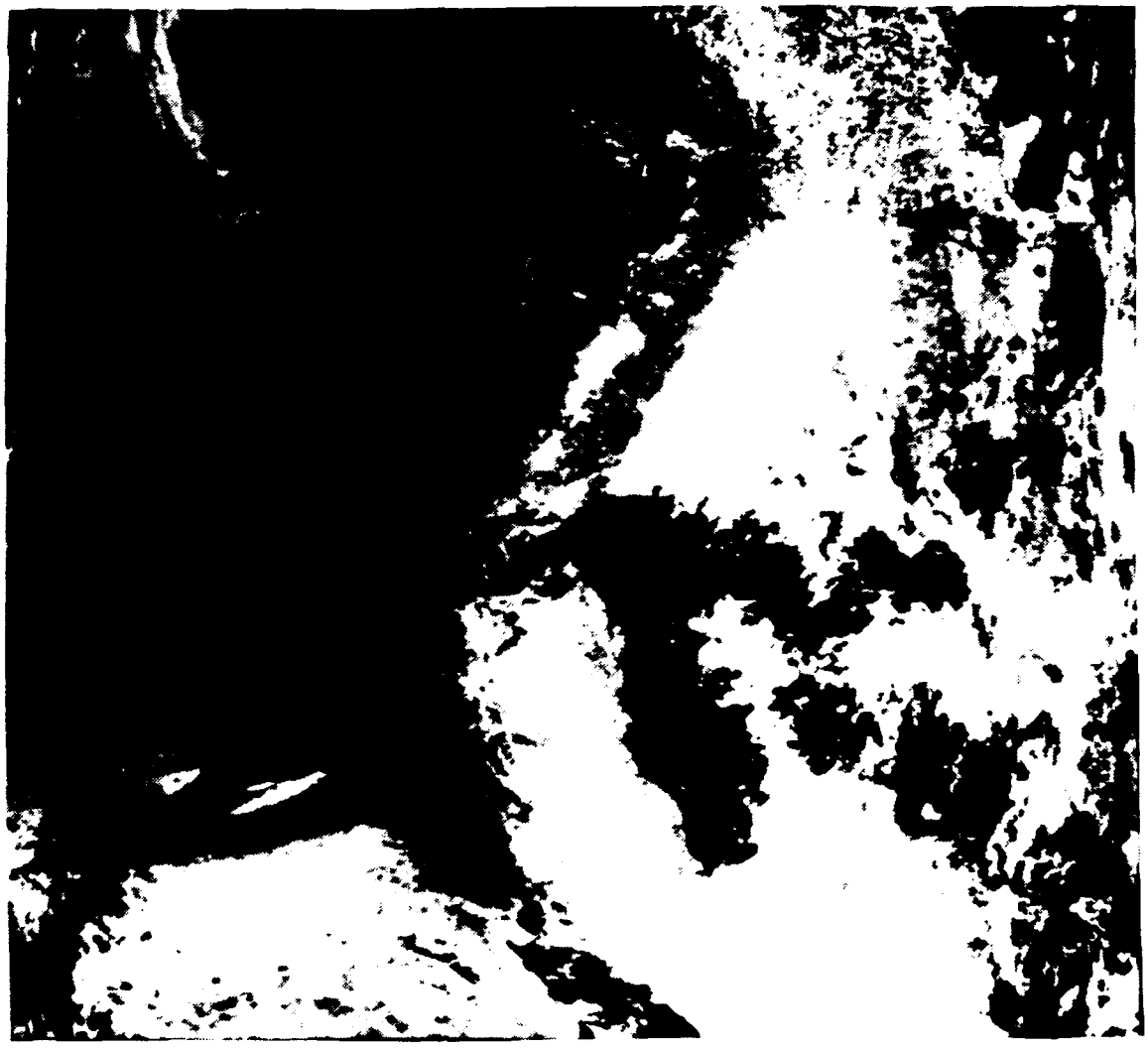

Figure 21. June 27, 1987 AVHRR channel 3 image

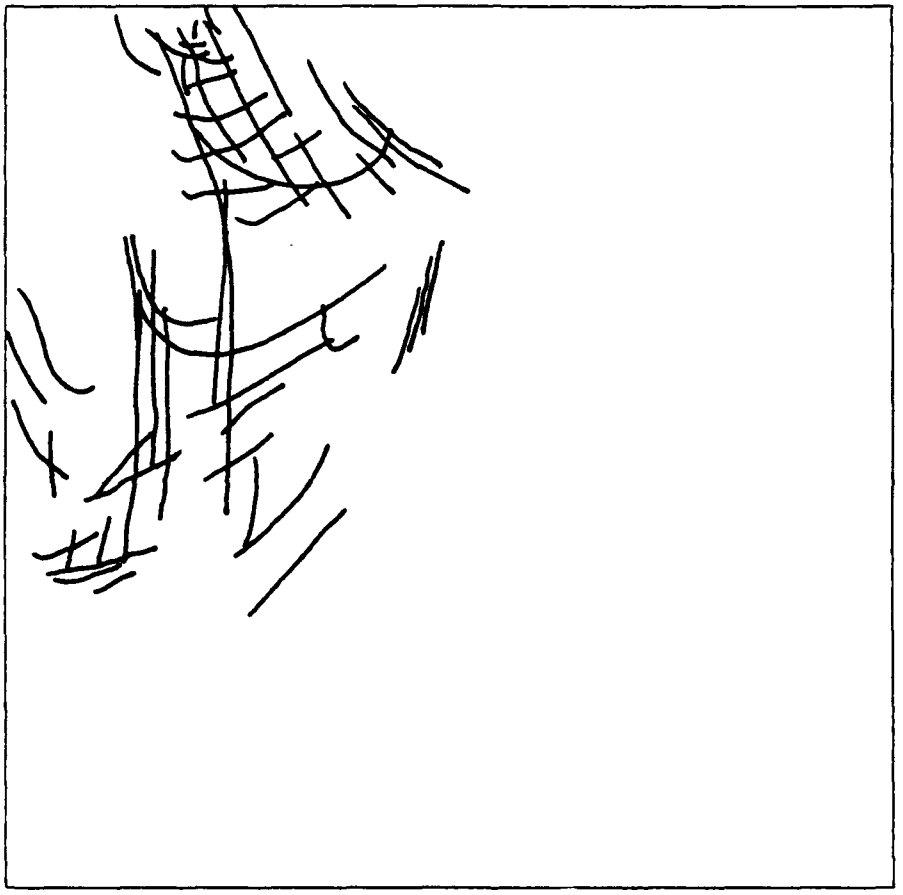

Figure 22. Subjective shiptrack analysis of June 27, 1987 pass

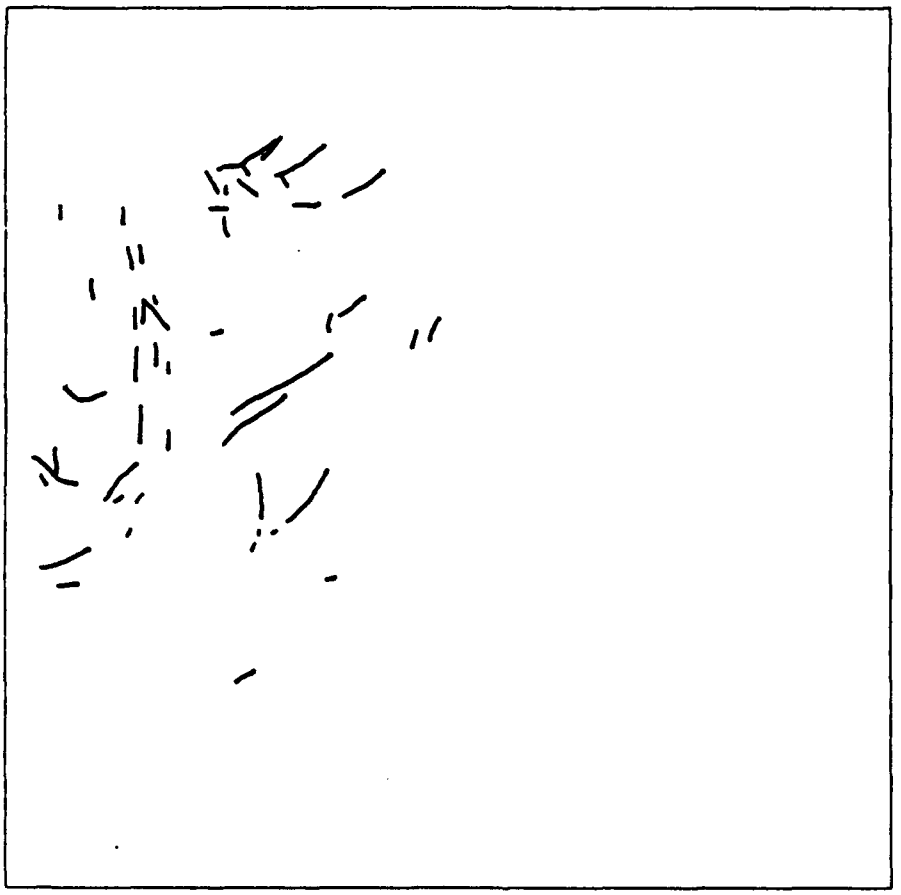

Figure 23. Algorithm Run A of June 27, 1987 pass.

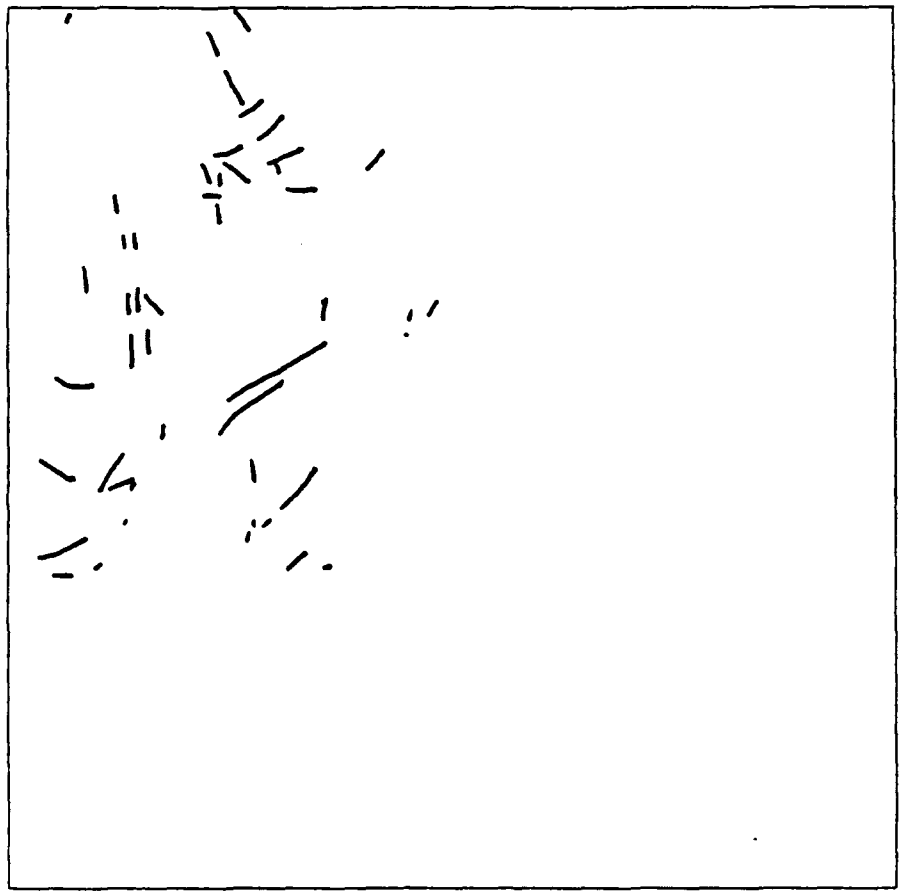

Figure 24. Algorithm Run B of June 27, 1987 pass.

TABLE 10
JUNE 27, 1987
SUBJECTIVE AND ALGORITHM
DETERMINED STATISTICS

SUBJECTIVE STATISTICS

NS = 52
NH = 44
ST = 15620
HL = 14400
OA =7.32

RUN A STATISTICS

STD = 27
HTD = 25
NHD = 15
STL = 3255
SHL = 3205
NFD = 6

RUN B STATISTICS

STD = 27
HTD = 24
NHD = 14
STL = 3035
SHL = 2925
NFD = 7

NS	=	Number of ST subjectively observed
NH	=	Number of HT subjectively observed
SL	=	Total length of observed ST
HL	=	Total length of observed HT
OA	=	Total open ocean area in $km^2 \times 10^6$
STD	=	Number of ST objectively detected
HTD	=	Number of HT objectively detected
NHD	=	Number of ST heads detected
STL	=	Total detected ST length
SHL	=	Total detected HT length
NFD	=	Number of false detections

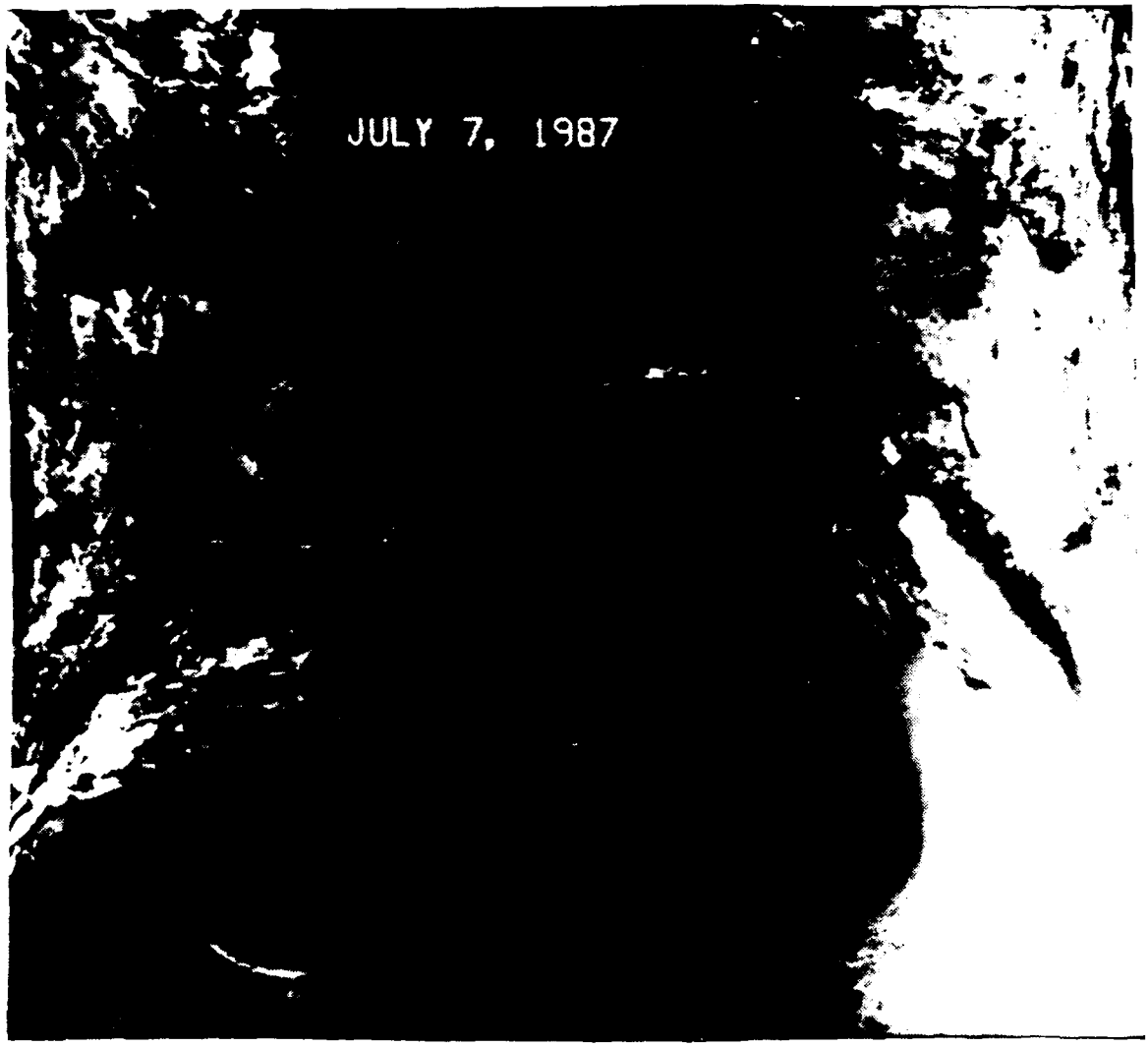

Figure 25. Northern half of July 7, 1987 AVHRR channel 3 image

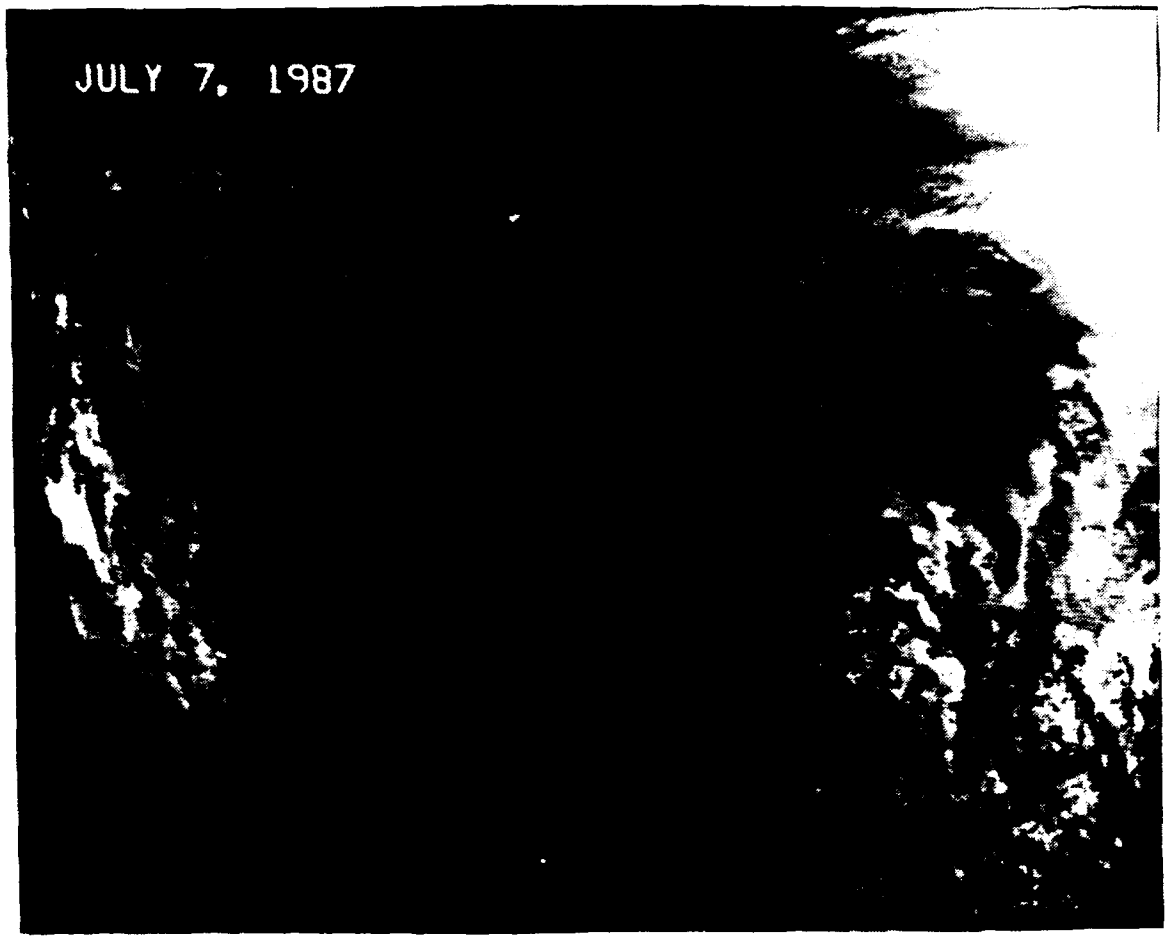

Figure 26. Southern half of July 7, 1987 AVHRR channel 3 image

Figure 27. Subjective shiptrack analysis of northern half of July 7, 1987 pass

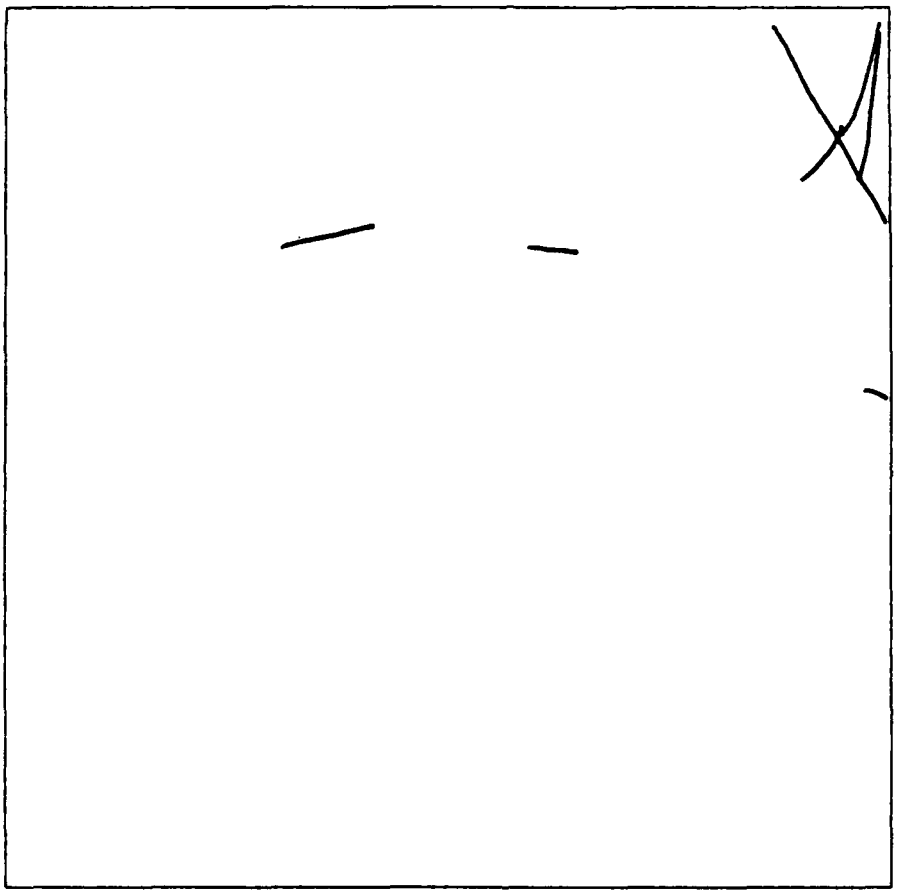

Figure 28. Subjective shiptrack analysis of southern half of July 7, 1987 pass

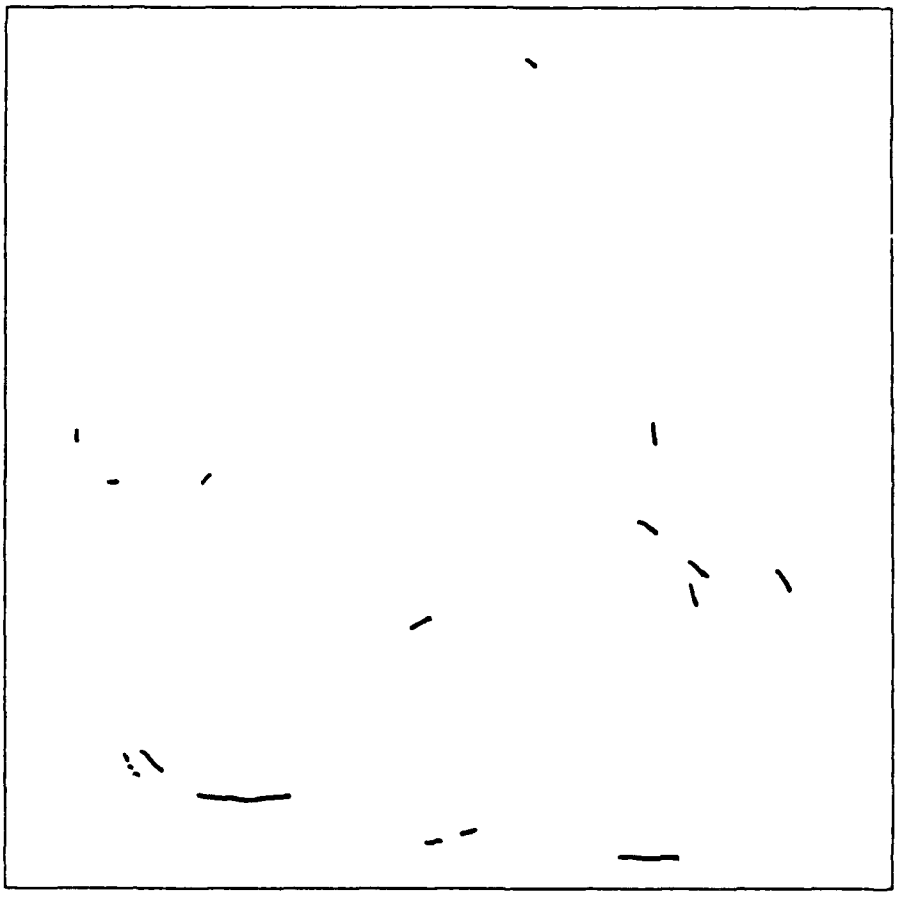

Figure 29. Algorithm Run A on northern half of July 7, 1987 pass.

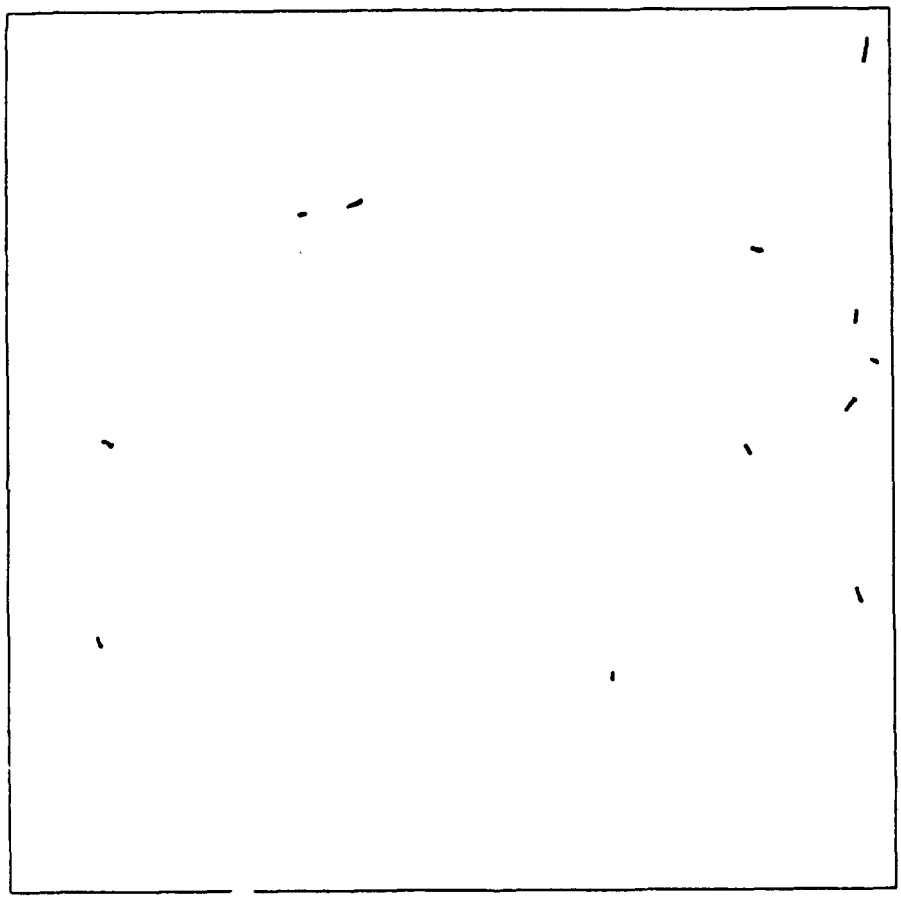

Figure 30. Algorithm Run A on southern half of July 7, 1987 pass.

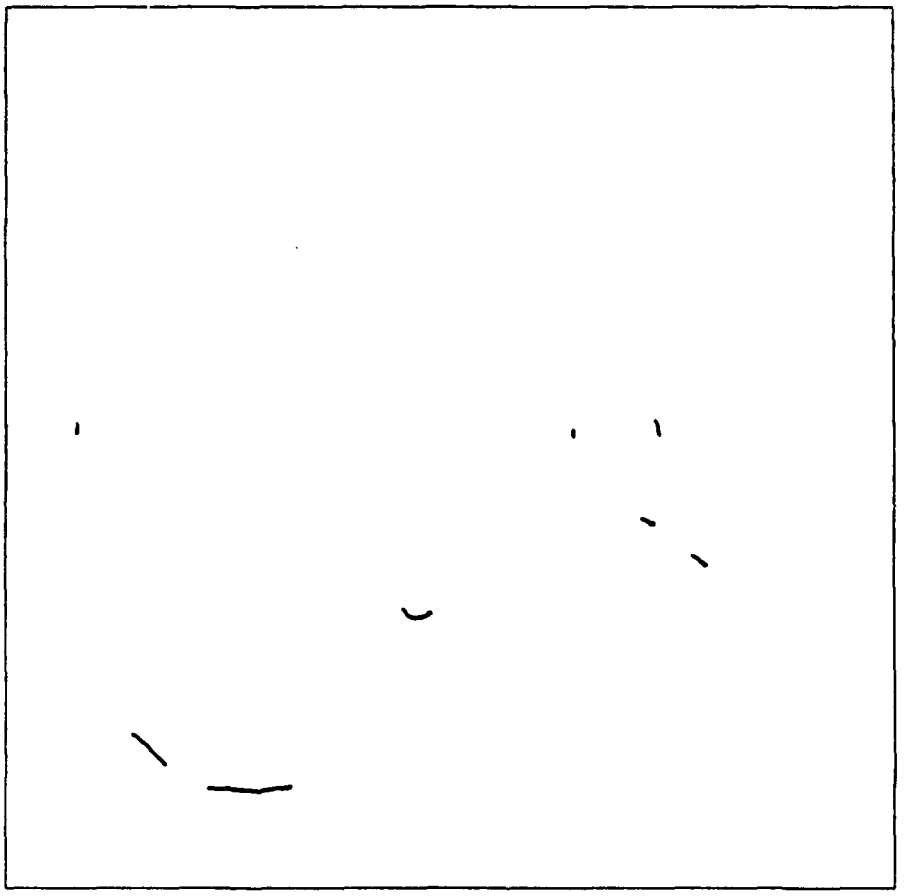

Figure 31. Algorithm Run B on northern half of July 7, 1987 pass.

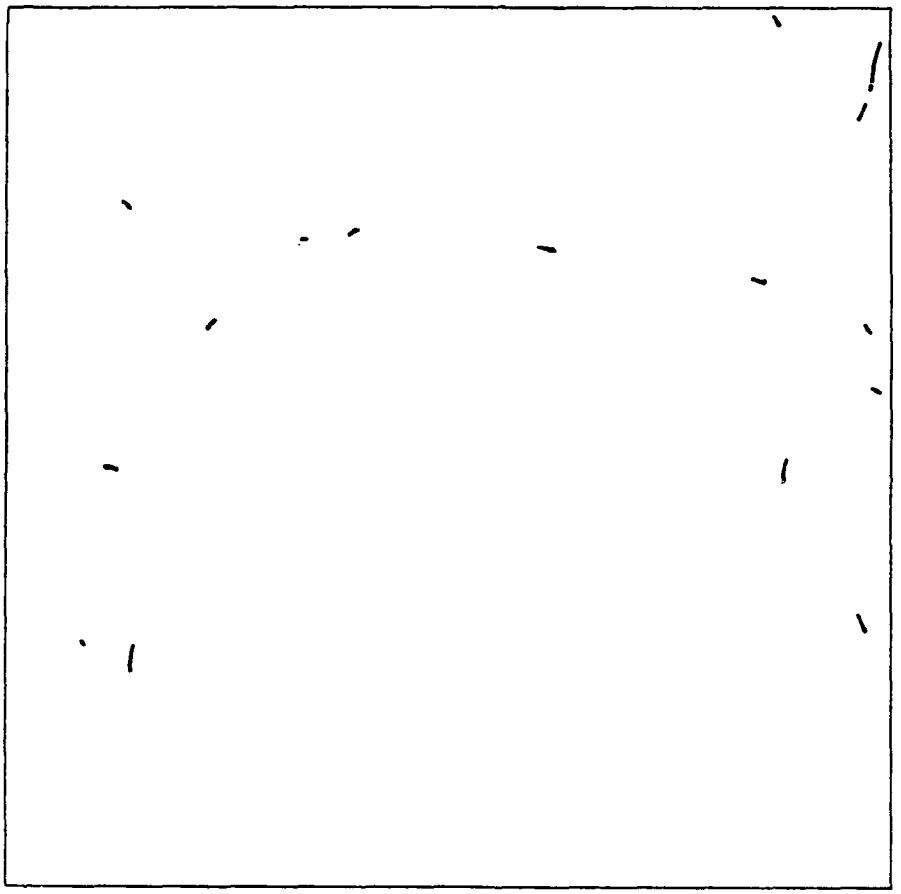

Figure 32. Algorithm Run B on southern half of July 7, 1987 pass.

TABLE 11
JULY 7, 1987
SUBJECTIVE AND ALGORITHM
DETERMINED STATISTICS

SUBJECTIVE STATISTICS

NS = 19
NH = 13
ST = 4610
HL = 3640
OA =8.35

RUN A STATISTICS

STD = 9
HTD = 6
NHD = 2
STL = 970
SHL = 840
NFD = 14

RUN B STATISTICS

STD = 8
HTD = 5
NHD = 2
STL = 940
SHL = 810
NFD = 12

NS	=	Number of ST subjectively observed
NH	=	Number of HT subjectively observed
SL	=	Total length of observed ST
HL	=	Total length of observed HT
OA	=	Total open ocean area in $km^2 \times 10^6$
STD	=	Number of ST objectively detected
HTD	=	Number of HT objectively detected
NHD	=	Number of ST heads detected
STL	=	Total detected ST length
SHL	=	Total detected HT length
NFD	=	Number of false detections

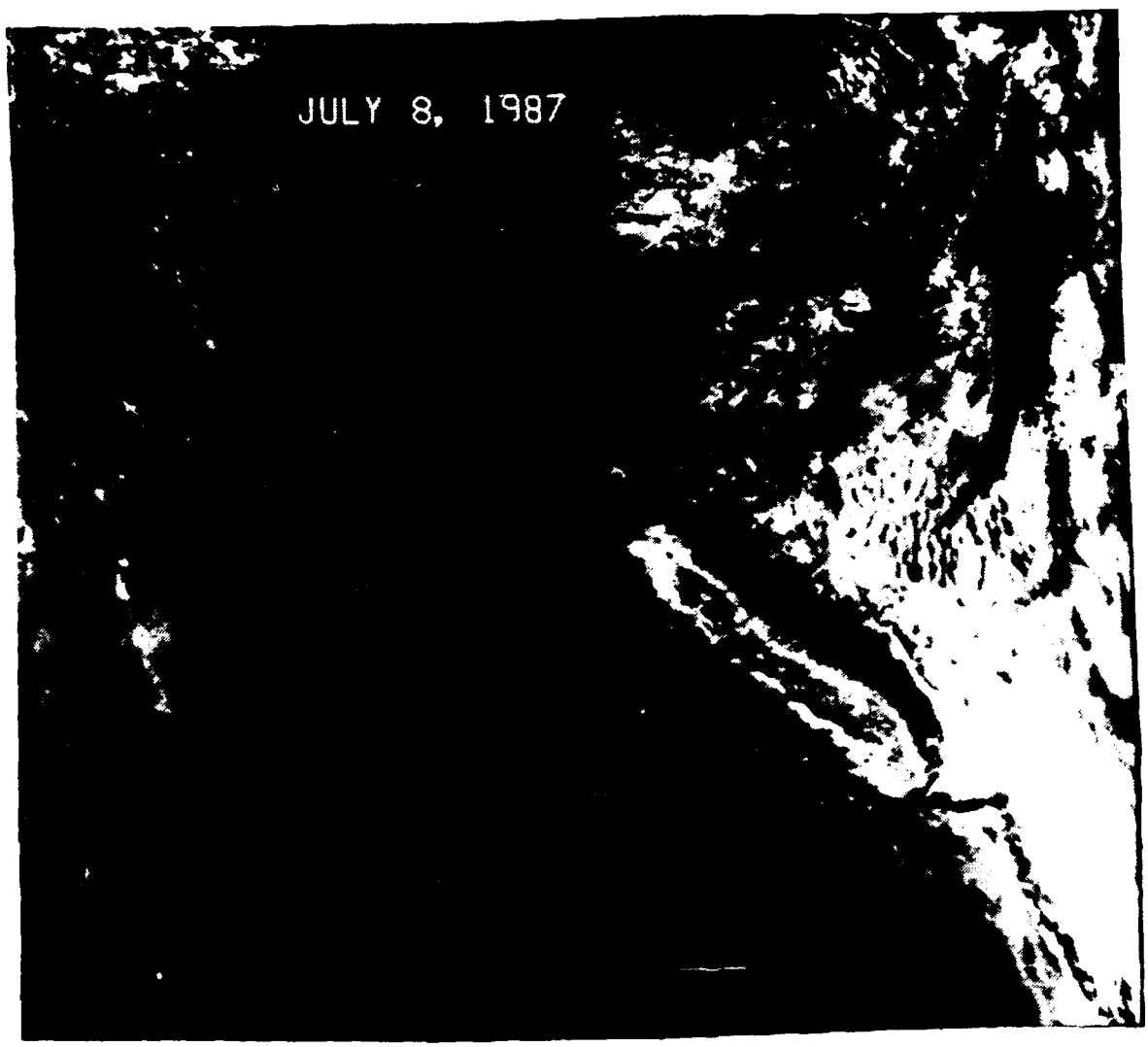

Figure 33. Northern half of July 8, 1987 AVHRR channel 3 image

Figure 34. Southern half of July 8, 1987 AVHRR channel 3 image

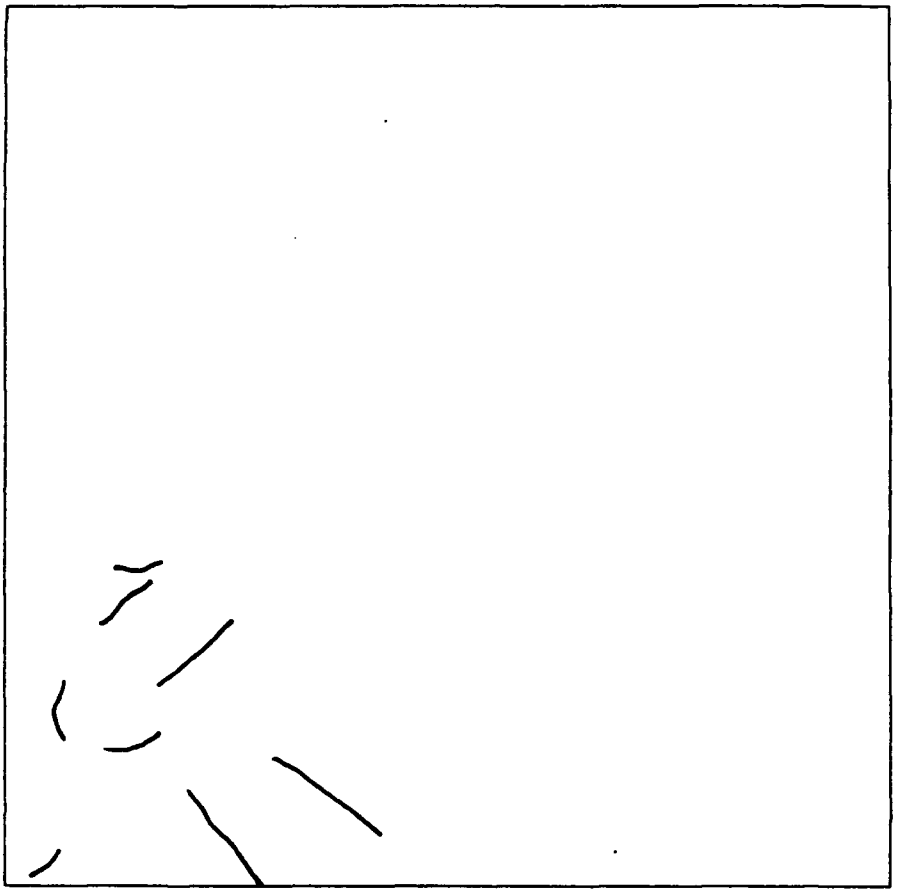

Figure 35. Subjective shiptrack analysis of northern half of July 8, 1987 pass

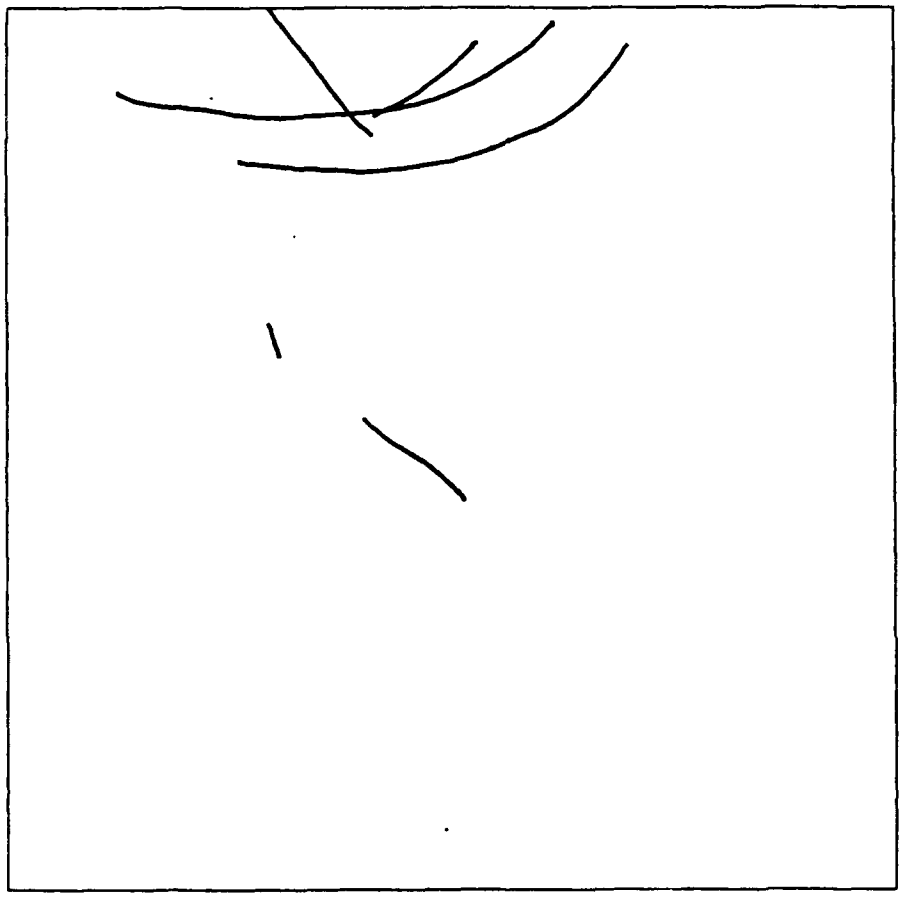

Figure 36. Subjective shiptrack analysis of southern half of July 8, 1987 pass

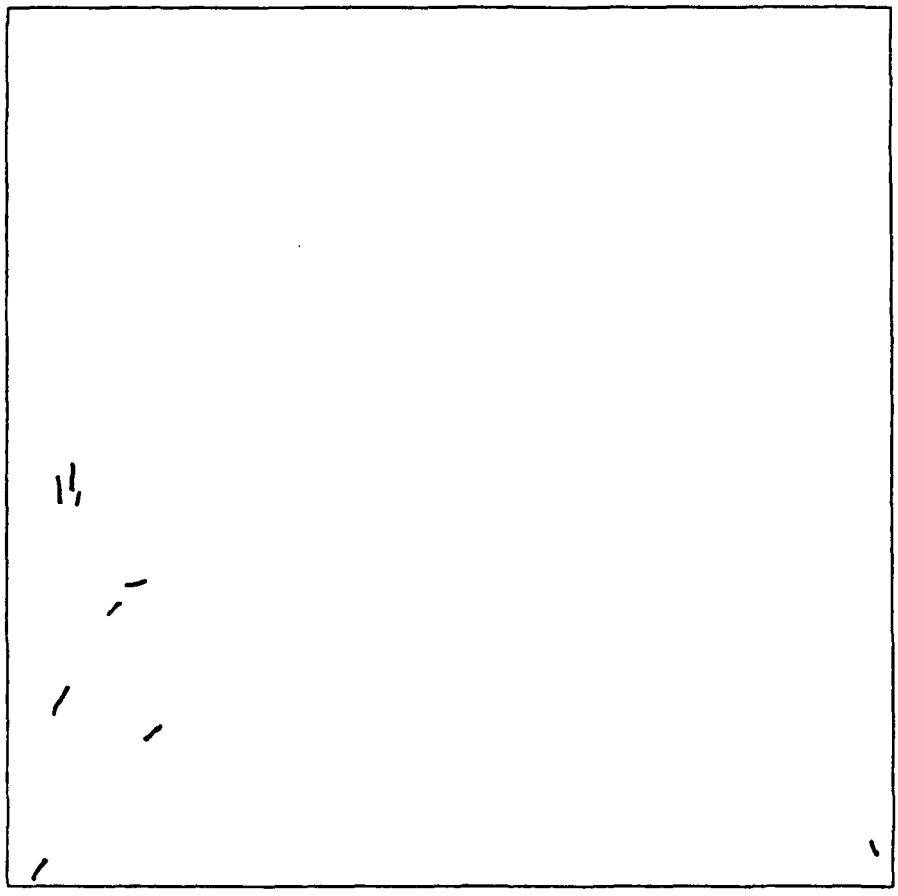

Figure 37. Algorithm Run A on northern half of July 8, 1987 pass.

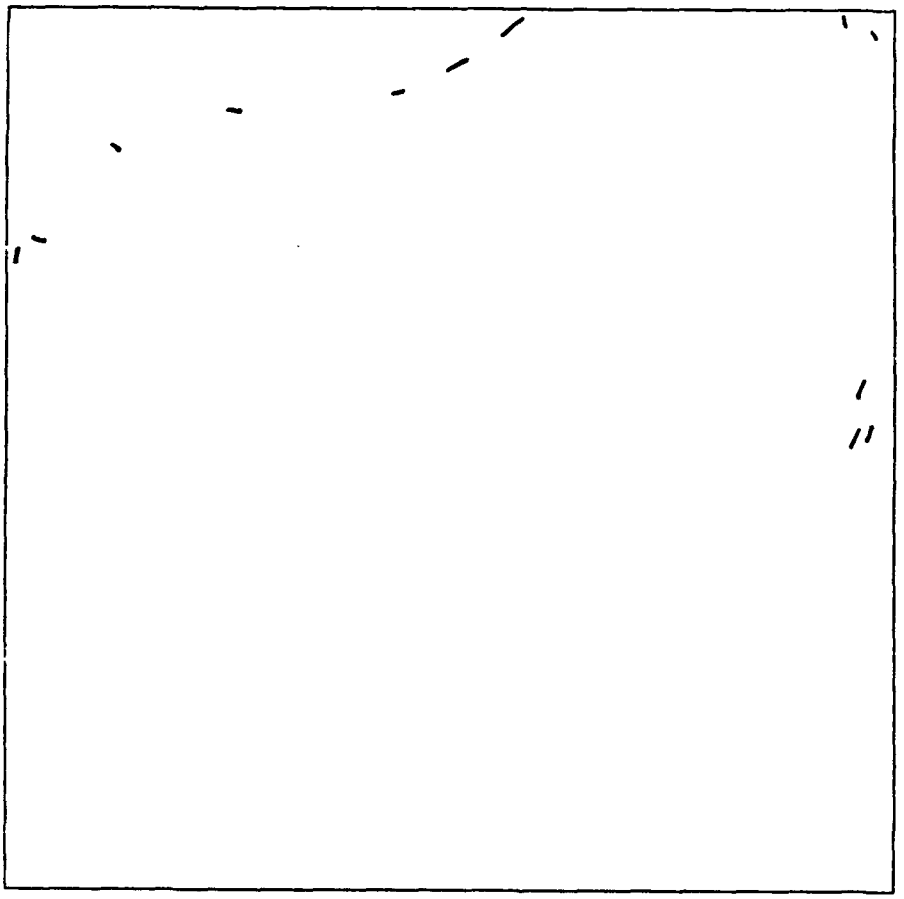

Figure 38. Algorithm Run A on southern half of July 8, 1987 pass.

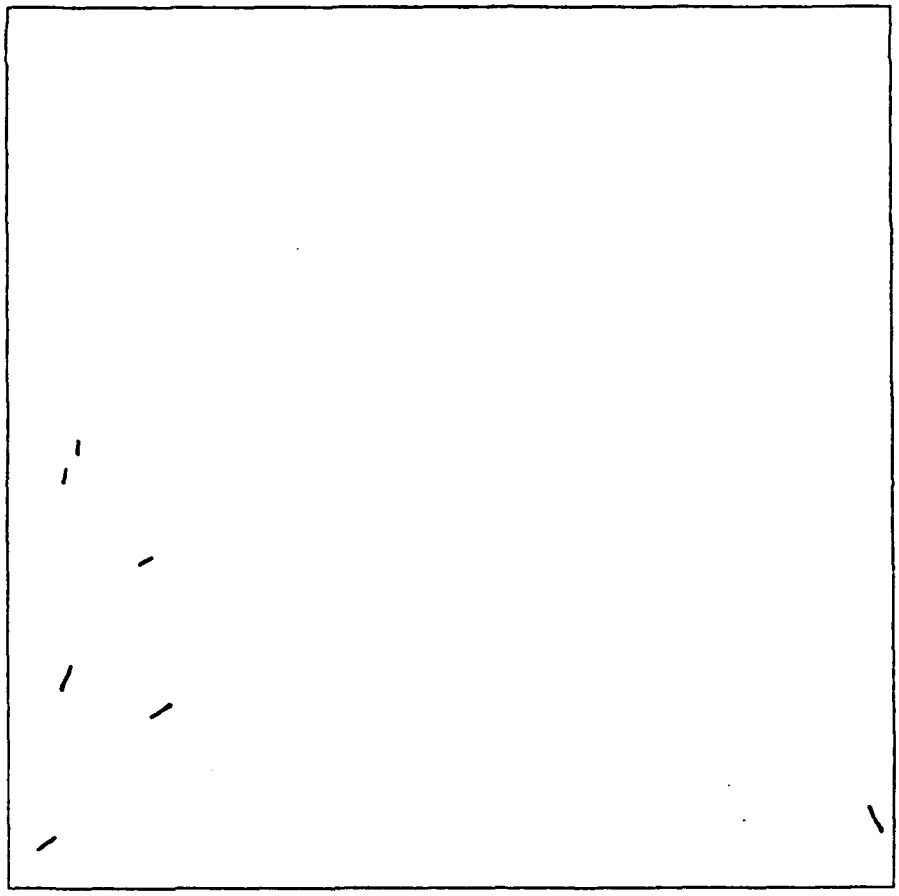

Figure 39. Algorithm Run B on northern half of July 8, 1987 pass.

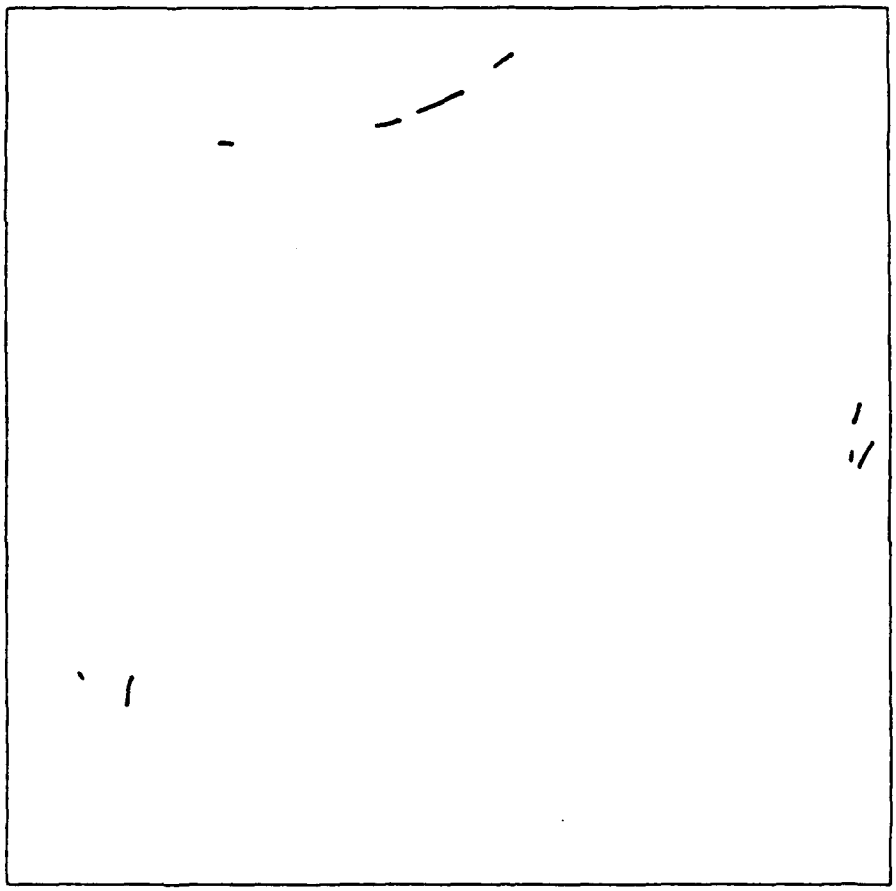

Figure 40. Algorithm Run B on southern half of July 8, 1987 pass.

TABLE 12
JULY 8, 1987
SUBJECTIVE AND ALGORITHM
DETERMINED STATISTICS

SUBJECTIVE STATISTICS

NS = 16
NH = 13
ST = 5725
HL = 5130
OA =5.55

RUN A STATISTICS

STD = 7
HTD = 4
NHD = 4
STL = 650
SHL = 300
NFD = 10

RUN B STATISTICS

STD = 6
HTD = 4
NHD = 4
STL = 695
SHL = 595
NFD = 5

NS	=	Number of ST subjectively observed
NH	=	Number of HT subjectively observed
SL	=	Total length of observed ST
HL	=	Total length of observed HT
OA	=	Total open ocean area in $km^2 \times 10^6$
STD	=	Number of ST objectively detected
HTD	=	Number of HT objectively detected
NHD	=	Number of ST heads detected
STL	=	Total detected ST length
SHL	=	Total detected HT length
NFD	=	Number of false detections

TABLE 13
ALGORITHM PERFORMANCE
STATISTICS

RUN A SETTINGS

Run	SR	HR	SL	HL	SC	FR	HD	FD
13JulA	72	91	38	55	72	28	70	1.31
LowA	63	83	31	35	74	26	57	1.07
27JunA	52	55	19	20	79	21	32	0.96
7JulA	47	46	21	23	39	61	15	1.68
8JulA	44	31	12	10	54	46	31	0.90
Combined	**57**	**65**	**25**	**26**	**63**	**37**	**43**	**1.31**

RUN B SETTINGS

13JulB	63	78	31	43	83	17	61	0.60
LowB	50	70	25	26	83	17	48	0.48
27JunB	52	57	21	22	82	18	34	0.82
7JulB2	42	38	20	16	40	60	23	1.44
8JulB	38	31	11	10	41	59	31	1.80
Combined	**51**	**58**	**22**	**23**	**72**	**28**	**39**	**0.87**

SR = *ST detection rate
HR = ◊STH detection rate
SL = ST length detection percentage
HL = STH length detection percentage
FR = False detection rate
SC = ST detection confidence
HD = Head detection rate
FD = False detections per $km^2 \times 10^6$

*ST denotes shiptrack
◊STH denotes shiptracks with clearly visible heads

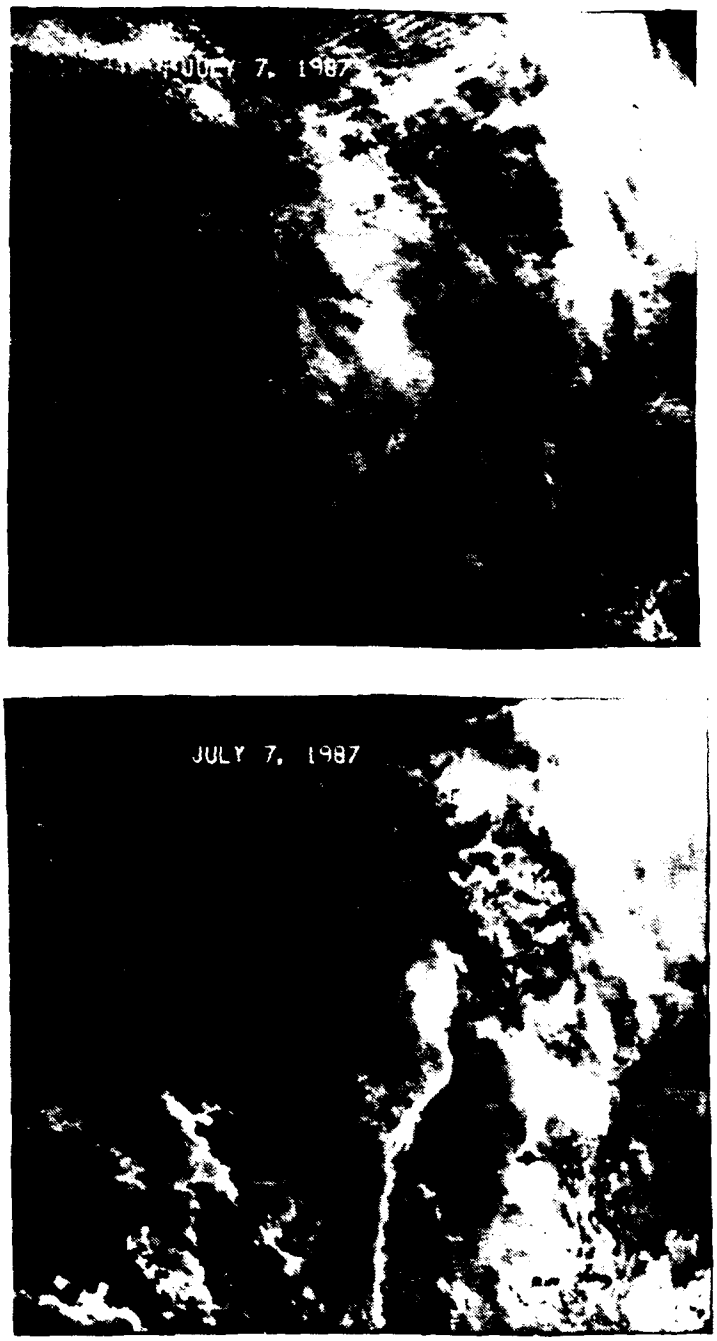

Figure 41. Natural cloud feature that produced algorithm false detections: North-south aligned cloud edge preferentially illuminated by the sun in the near-IR in a low sun angle region of the July 7 pass. Top image is channel 1. Bottom image is channel 3.

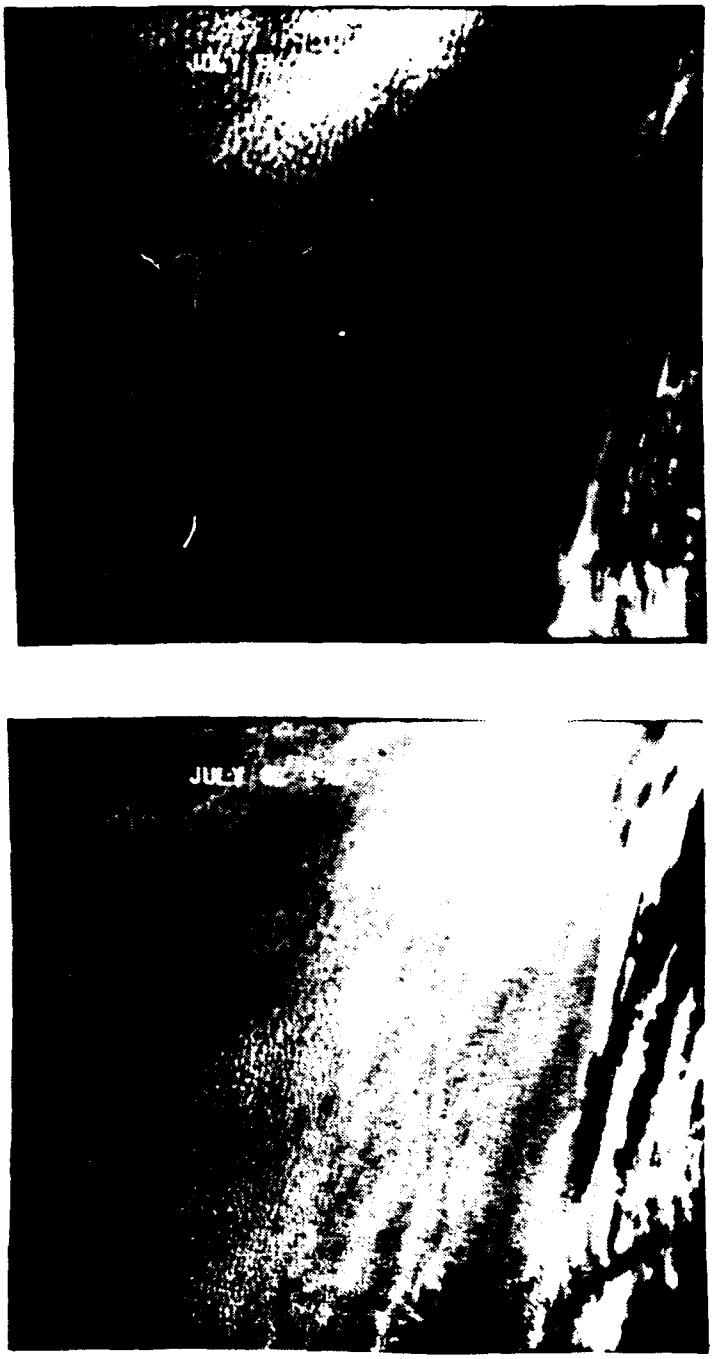

Figure 42. Natural cloud feature producing algorithm false detections: Relatively thin cloud streaks over water near the edge of the July 13 pass. Top image is channel 1. Bottom image is channel 3

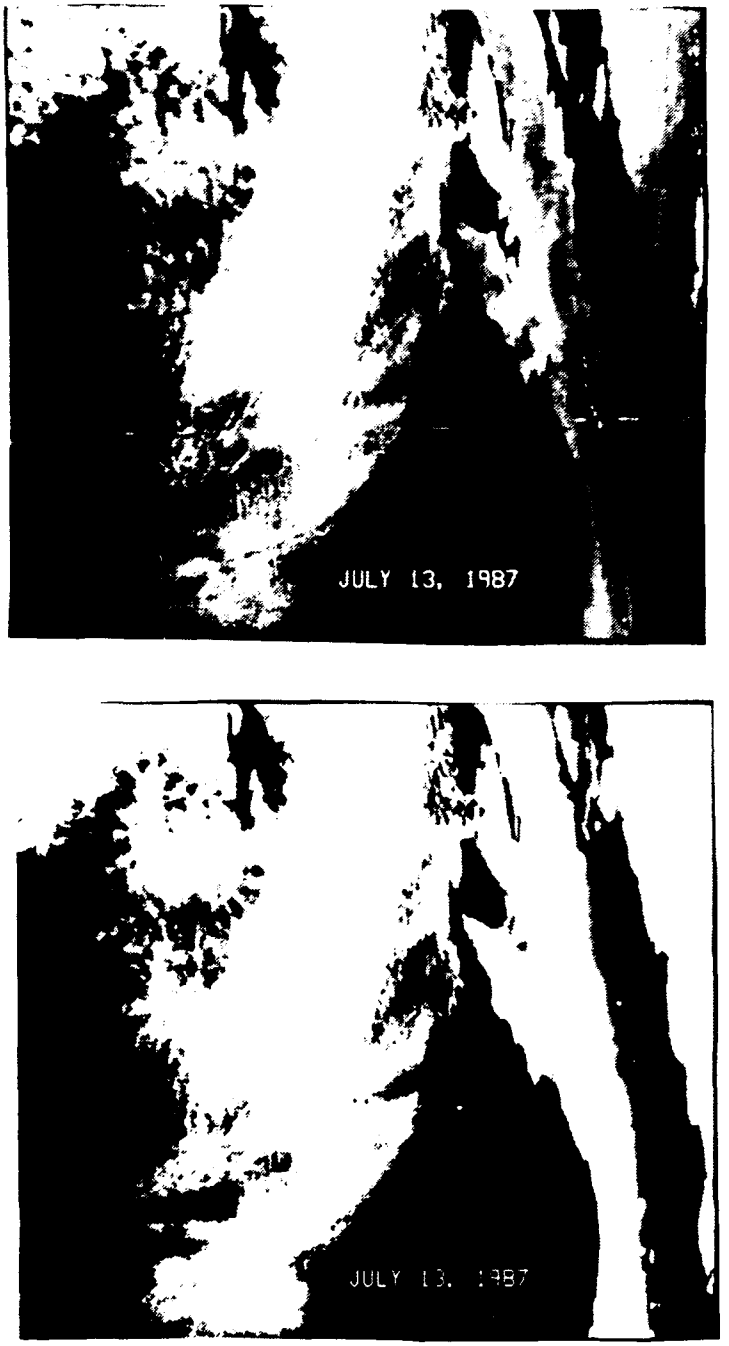

Figure 43. Natural cloud feature producing algorithm false detections: Gravity wave interaction with marine boundary layer. Top image is channel 1. Bottom image is channel 3

VI. CONCLUSIONS AND RECOMMENDATIONS

The goal of this project was to quantitatively determine the performance of the most recent version of a shiptrack detection algorithm. The statistics are prepared from the author's subjective analysis of the four satellite passes. Many times during the subjective analysis, a feature that possessed all the right shiptrack characteristics in terms of channel 1, 3 and 4 brightness, gradients and temperatures, was rejected simply because it didn't *look* like a shiptrack. Clearly, this subjectivity must be taken into account when reviewing absolute numbers describing the algorithm's performance.

Overall, the algorithm performed as designed, detecting the majority of the shiptracks without producing excessively high numbers of false detections. The performance characteristics of the two chosen "optimum" control parameter settings fluctuated from pass to pass, generally performing better on those cases having a large number of bright shiptracks (July 13 and June 27) than those with less bright and fewer shiptracks (July 7 and 8). Run A settings consistently detected a higher number of shiptracks than Run B settings but consistently produced a higher false detection rate.

The low3 version of the July 13 case was less successful than the original channel 3 version. In the near-IR, the low3 image did not show the shiptracks as well as the channel 3 image. The cause for this difference is not clear and deserves further study.

A. FALSE DETECTIONS

Much can be learned from a closer examination of algorithm false detections. In every case, of course, features causing false detections fit the coded description of shiptracks. In each case the feature was subjectively rejected as fitting into one or more of the categories of naturally occurring cloud line features. With further research, it may be possible to find specific characteristics in common to many of these the features (but not common to shiptracks in general) and use characteristics to build specific filters into the algorithm designed to reject these naturally occurring features, Once in place, these filters would allow the acceptance parameters within the algorithm to be more relaxed, thus allowing more potential shiptracks to get through to the filters. Building more efficient filters and testing more potential shiptrack path segments would enhance the performance of the algorithm.

B. ALGORITHM MODIFICATIONS

There are many places within the code where empirical limits govern how shiptracks are defined and how they are tested. One such place is within the subroutine *Pave*, where the shiptrack path is defined to be 7 pixels wide and is compared to regions in the adjacent cloud field as part of the subroutine's acceptance tests. This approach generally fails towards the tail region of a shiptrack where the cloud line becomes significantly wider than 7 pixels or near the head where it may be less than the maximum resolution of the image (1.1 km).

An alternate approach to this particular problem is to define the shiptrack path as the region within the minimum and maximum channel 3 gradients as apposed to an arbitrary constant width. Such an approach would decrease the number of tests needed in *Pave* to one simple requirement that the path be brighter than the adjacent cloud field. This idea is presently in the testing phase and looks promising.

A second proposal is increasing the maximum allowable path segment length to approximately 100 km and incorporating variable *Pave, Gravel* and *Landscape* path perpendicular percentages based on path segment length. This may allow a greater percentage of longer shiptracks to be detected without sacrificing discriminating tests on the shorter features.

The continuing study of objective shiptrack detection will aid in the analysis of the shiptrack phenomenon and lead to a better understanding of the modification of oceanic stratus clouds.

LIST OF REFERENCES

Allen, R. C., Jr. 1987: Automated satellite cloud analysis: A multispectral approach to the problem of snow/cloud discrimination. M. S. thesis, Naval Postgraduate School, Monterey, CA, May 1987, 66 pp.

Coakley, J. A., Jr., R. L. Bernstein and P. A. Durkee, 1987: Effect of ship stack effluents on cloud reflectivity, *Science,* **237**, 953-1084.

Conover, J. H., 1966: Anomalous cloud lines. *J. Atmos. Sci.*, **23**, 778-785.

Durkee, P. A., and J. Lutz, 1991: Frequency of occurrence of ship tracks in the eastern North Pacific Ocean. In preparation.

Hindman, E. E., 1990: Understanding ship-trail clouds. Preprints of 1990 conference on cloud physics, July 23-27, 1990, San Francisco, California, AMS, Boston, MA, 1990.

Neilsen, K. E., 1991: A robust algorithm for locating ship track cloud features using 3.7 micron satellite data. Unpublished.

Radke, L. F., J. A. Coakley, Jr. and M. D. King, 1989: Direct and remote sensing observations of the effects of ships on clouds. *Science*, 246, 1146-1148.

Rao, P. K., S. J. Holmes, R. K. Anderson, J. S. Winston and P. E. Lehr, Editors: *Weather Satellites*, pp161-162, 453, American Meteorology Society, 1990.

INITIAL DISTRIBUTION LIST

		No. Copies
1.	Defense Technical Information Center Cameron Station Alexandria, VA 22304-6145	2
2.	Library, Code 52 Naval Postgraduate School Monterey, CA 93943-5000	2
3.	Chairman (Code MR/Hy) Department of Meteorology Naval Postgraduate School Monterey CA 93943-5000	1
4.	Chairman (Code OC/Co) Department of Oceanography Naval Postgraduate School Monterey, CA 93943-5000	1
5.	Professor Philip A. Durkee (Code MR/De) Department of Meteorology Naval Postgraduate School Monterey, Ca 93940-5000	1
6.	Professor Carlyle H. Wash (Code MR/Wx) Department of Meteorology Naval Postgraduate School Monterey, CA 93943-5000	1
7.	Kurt Nielsen (Code MR/Ne) Department of Meteorology Naval Postgraduate School Monterey, CA 93943-5000	1
8.	LT. Vincent F. Giampaolo 23836 Birch Lane Mission Viejo, CA 92691	2

9. Director Naval Oceanography Division — 1
Naval Observatory
34th and Massachusetts Avenue NW
Washington, DC 20390

10. Commander — 1
Naval Oceanography Command
Stennis Space Center
MS 39529-5000

11. Commanding Officer — 1
Naval Oceanographic Office
Stennis Space Center
MS 39522-5001

12. Dr. Gary L Geernaert — 1
Office of Naval Research
Arlington, VA 22217